

We are IntechOpen, the world's leading publisher of Open Access books Built by scientists, for scientists

6,900

Open access books available

186,000

International authors and editors

200M

Downloads

Our authors are among the

154

Countries delivered to

TOP 1%

most cited scientists

12.2%

Contributors from top 500 universities



WEB OF SCIENCE™

Selection of our books indexed in the Book Citation Index
in Web of Science™ Core Collection (BKCI)

Interested in publishing with us?
Contact book.department@intechopen.com

Numbers displayed above are based on latest data collected.
For more information visit www.intechopen.com



Desktop Robot Based Rapid Prototyping System: An Advanced Extrusion Based Processing of Biopolymers into 3D Tissue Engineering Scaffolds

M. Enamul Hoque and Y. Leng Chuan
*University of Nottingham Malaysia Campus
Malaysia*

1. Introduction

Since ancient times, tissue repair has been the ultimate goal of surgery. Tissue engineering is a technique to regenerate tissues and organs. It involves in vitro seeding and attachment of cells onto a scaffold. These cells then proliferate, migrate and differentiate into the intended specific tissue. The appropriateness of scaffold is essentially crucial to enable the cells to behave in the required manner producing tissues and organs of the desired shape and size. A key issue concerning the tissue engineering scaffold fabrication is the development of processing techniques flexible to building materials to fabricate scaffolds with biocompatibility and mechanical properties as close as local tissues. These techniques must also have the capability of producing adequate porosity in the scaffold to further serve as a framework for cell penetration, new tissue formation, and subsequent remodelling. Therefore, in the design of tissue engineering scaffolds, the characteristics that include pore size, shape, porosity, interconnectivity, and bio-mechanical properties should be optimized to maximize successful inducement of tissue in growth. Conventional scaffold fabrication techniques mostly focus on producing foam like structure from polymeric materials. The limitations of conventional techniques include the lack of structural stability and pore connectivity in the developed scaffolds. With continual advancement of scaffold-based tissue engineering therapies, an increased attention has been paid to the challenges in designing and developing patient-specific 3D scaffolds. Rapid prototyping (RP) technology in combination with synthetic biopolymer could be an up-to-date solution to the challenges in developing appropriate scaffolds in need. RP technology uses layer-manufacturing strategy to build 3D scaffold directly from computer-generated models. It can improve current scaffold design by controlling scaffold parameters such as filament diameter, filament gap and lay-down pattern. These pore scale parameters are correlated to the porosity, pore connectivity and mechanical stability of the scaffolds. This chapter presents the scaffold-based tissue engineering approach, scaffold functions & requirements, materials for scaffolds and scaffold fabrication techniques. In addition, an evaluation study of the scaffolds developed by desktop robot based rapid prototyping (DRBRP) system is reported.

2. Scaffold-based tissue engineering

The loss or failure of an organ or tissue is one of the most frequent, devastating and costly problems in healthcare services. Current treatment modalities for diseased or damaged organs include transplantation, surgical reconstruction, use of mechanical devices, or supplementation of metabolic products (Sonal, 2001). However, these therapies remain insufficient due to lack of donors and regaining functionality of the reconstructed organs.

Tissue engineering is an interdisciplinary field that brings together the principles of life sciences, medicine and engineering to develop functional artificial tissues to maintain, improve or replace lost or damaged tissue/organ (Lacroix & Prendergast, 2002; Maher et al., 2009). This technology produces physiologic 'replacement parts' for impaired tissues or organs which restore, maintain or improve the function of patient's tissues (Lacroix & Prendergast, 2002) (see Fig. 1.). The implantation of engineered biological substitute will be functional either at the time of implantation, or integrate and form the expected functional tissue at a later stage (Joseph & Robert, 1999; Joseph, 2006).

Tissue engineering requires a mechanically stable, biocompatible, and biodegradable scaffold that allows cell adhesion and proliferation, permits preservation of cell specific properties, and suitable for surgical implantations (Joseph, 2006; Moroni et al., 2006). Therefore, fabricated scaffold should mimic the biomechanical properties of the organ or tissue to be replaced as closely as possible. To meet such requirements, development of appropriate 3D scaffold for tissue construction remains a great challenge in various tissue engineering areas.

There are specific shortcomings on developing different types of tissue engineering scaffolds. For example, current scaffolds for skin tissue engineering are not ideal because they are unable to provide optimal environment for cell adherence, proliferation, and multiplication (Joseph & Robert, 1999). Bone tissue has the capacity of self reconstruction upon injury. However, when the defect is remarkably large it usually remains unrepaired and requires an ideal filler, such as cadaver bone, coral, hydroxyapatite or similar mineral compounds (Pinar et al., 2008). Nevertheless, cartilage always has poor cell density and lack of vascularisations that make the cartilage difficult to be repaired, and leads to the use of an appropriate scaffold (Lebourg et al., 2008).

Three general strategies have been recommended for developing new tissue (Tezcaner et al., 2002). They are as follows:

1. **Isolated cells or cell substitutes:** This approach avoids the complications of surgery, allows replacement of only those cells that supply the needed function, and permits manipulation of cells before infusion. However, its potential limitations include the failure of infused cells to maintain their functionality in the recipient, and immunological rejection.
2. **Tissue-inducing substances:** The success of this approach depends on the purification and large-scale production of appropriate signal molecules, such as growth factors, and in many cases, the development of methods to deliver these molecules to their targets.
3. **Cells placed on or within matrices:** In closed systems, the cells are isolated from the body by a membrane that allows permeation of nutrients and wastes but prevents large entities such as antibodies or immune cells from destroying the transplant. These systems can be implanted or used as extracorporeal devices. In open systems, cells attached to matrices are implanted and incorporated into the body. The matrices are fashioned from natural or synthetic polymers.

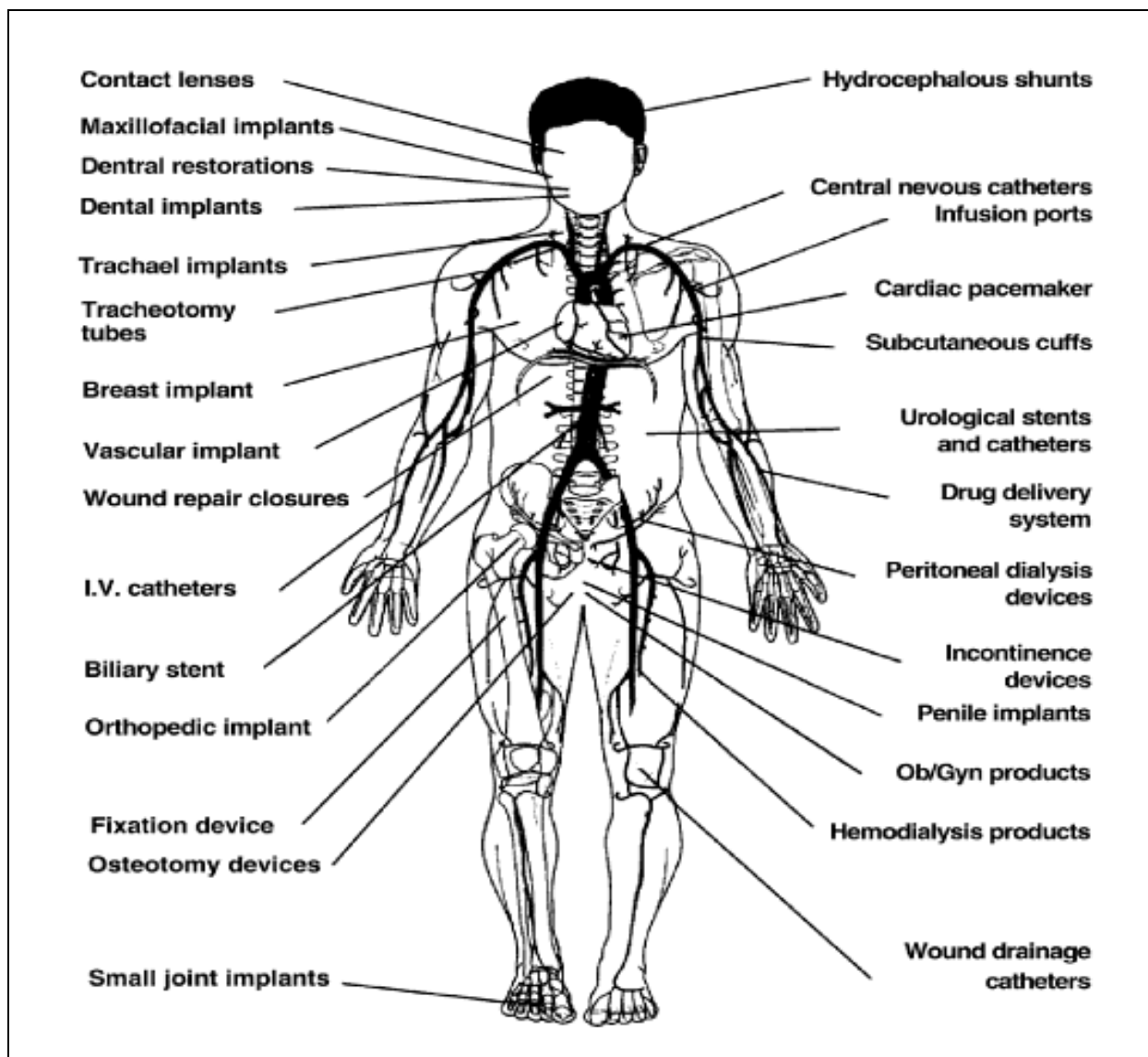


Fig. 1. Illustrations of various implants and devices used to replace or enhance the function of diseased or damaged tissues and organs (Park & Lakes, 2007)

For scaffold-based therapy, tissue engineering new treatment method is investigated for the reconstruction of large bone defects, where cells are taken from the patient or a donor, cultured in-vitro and seeded in a scaffold. The scaffold along with cells is then implanted in the defect with the aim to stimulate new bone formation, thereby repairing the defect. This approach delivers promising results not only for bone tissue, but also for other organs and tissues (Van et al., 2006).

The general techniques applied in the design of scaffolds include cell-seeded polymeric scaffolds, cell-seeded gels, and cell self-assembly into a cellular matrix (Ke & William, 2010). Cell-seeded polymeric scaffolds are the most commonly used method in the artificial tissue generation, and many scientists consider this technique as the classic tissue engineering approach. It involves the production of a scaffold into or onto which cells are placed, allowing them to organize into a 3D assembly having similar characteristics as natural cell-extracellular matrix arrangements and interactions (Frisman et al. 2010) (see Fig. 2).

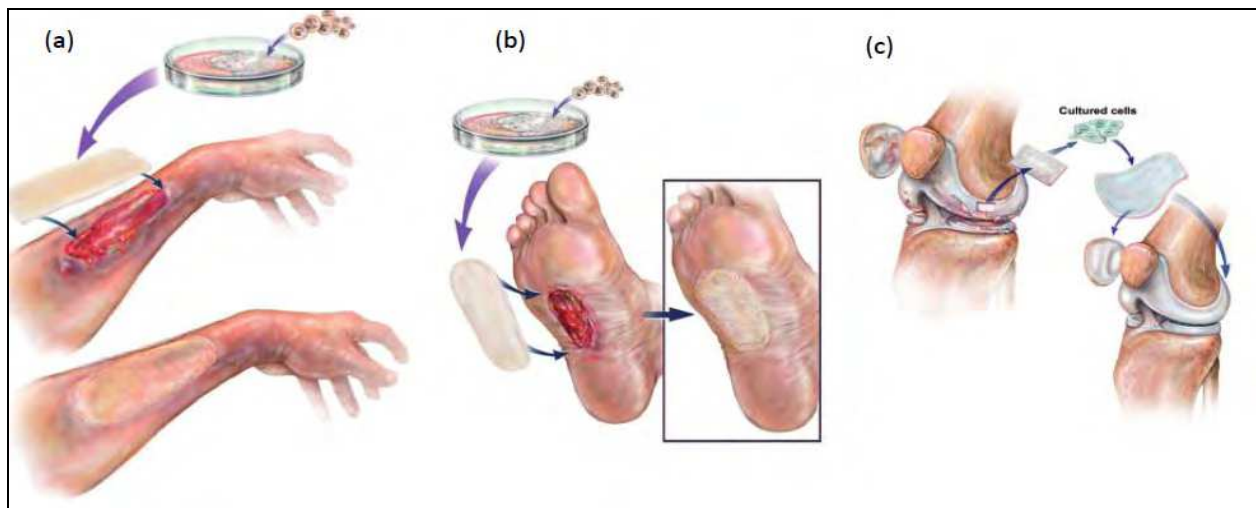


Fig. 2. Orthobiological approaches to (a) & (b) clinical skin remodelling using autologous cell-based therapies, (c) patient-specific cartilage replacement therapy based on collagen and/or extracellular matrix (Lanza et al., 2007)

3. Scaffold functions and requirements

In the success of tissue engineering, 3D scaffold plays important role as extracellular matrix onto which cells can attach, grow and form new tissues (Badylak, 2007). The primary functions of scaffold are (Kim, 2001):

- To serve as an adhesion substrate for the cell, facilitating the localization and delivery of cells when they are implanted.
- To provide temporary mechanical support to the newly grown tissue by defining and maintaining a 3D structure.
- To guide the development of new tissues with the appropriate function.

Fabricated scaffold should mimic the biomechanical properties of the organ or tissue to be replaced, and possess following principal characteristics (Leong, 2003; Hollister et al., 2002):

- Simulate the microstructure as similar as possible to that of native tissue.
- Have a suitable macrostructure to promote cell proliferation and cell-specific matrix production.
- Provide a temporary support and function while cells regenerate.
- Being made from a material with a predictable rate of degradation with nontoxic degraded by-product(s).
- Made of open-pore geometry with a highly porous surface and microstructure that enables cell in growth.
- Optimal pore size employed to facilitate cellular permeation, encourage tissue regeneration and to avoid pore occlusion.
- Having suitable surface morphology and physiochemical properties to encourage intracellular signalling and recruitment of cells.

There is always a great challenge in modelling, design and fabrication of tissue engineering scaffold to meet the required biological and biophysical conditions to regenerate tissues. For example, designing load bearing scaffolds for bone and cartilage tissue applications (Holland & Tighe, 1992; Badylak, 2007; Drury & Mooney, 2003) is a complicated process. Bone and cartilage tissue scaffolds usually have complex architecture, porosity, pore size,

shape and interconnectivity in order to provide the needed structural integrity, strength, transport, and an ideal micro-environment for the growth of cells and tissues in growth (Sun et al., 2005).

There is tremendous need to assess how the exact match of mechanical properties of scaffolds with the native organ is crucial for optimal tissue regeneration. For instance, since mechanical properties are intimately related to the porosity of porous structures, whether a stiffer and less porous scaffold will provide a better integration with the surrounding natural tissue, or a more flexible and porous one will allow cells to attach and proliferate in a more efficient way (Zhensheng et al., 2008; Tjong, 2006; Puppi et al., 2010).

4. Materials for scaffolds

There is a broad list of bulk materials currently used in the fabrication of tissue engineering scaffolds. These include tissue-derived materials, biological polymers, ceramics or mineral-based matrices, metals and composites of two or more materials (Griffith and Grodzinsky, 2001) (Table 1.). The biodegradable polymers are suitable for many commercial products and medical applications, such as packaging, surgical implants, controlled release and drug delivery systems. However, their uses are still limited due to their high cost and/or low performances.

Materials	Example
Tissue-derived materials	Allograft bone matrix, skin and intestinal submucosa
Biopolymers	Collagen, hyaluronan, fibrin and alginate
Ceramics	Tricalcium phosphate, hydroxyapatite and calcium sulfate
Metals	Titanium, tantalum and other alloys

Table 1. Materials used in the fabrication of tissue engineering scaffold

Continuous research is going on in the field of biomaterials to fulfil the broad need of potential tissue engineering applications. New materials should possess particularly desirable tissue-specific properties, which should have broad applicability and can be tailored to several tissue systems (Madihally & Matthew, 1999). A material that can be used as a scaffold in tissue engineering must satisfy a number of requirements. These include biocompatibility, controlled biodegradation within the time frame required for the application and production of non-toxic products, processability to complicated shapes with appropriate porosity, ability to support cell growth and proliferation, and appropriate mechanical properties as well as maintaining mechanical strength during tissue regeneration process (Gunatillake & Adhikari, 2003). Besides, the selection of material used in the manufacture of a tissue engineering scaffold is dependent on the proposed tissue type, processing technique employed and its intended application (Thomson et al., 2000; Leong et al., 2003).

The polymer's design and processing flexibility influence its choice to be used as a biomaterial (Melchels et al. 2010; Harley et al., 2008). Medical fields have been targeting to employ biopolymers in every aspect for many years. Polymer can be chemically modified to match a wide range of properties in biomedical applications, such as mechanical properties, diffusivity, density, hydrophilicity, etc. By using polymeric material, there can be optimal control over specific cellular interactions with the scaffold material because, cells do not interact with proteins that are attached to some polymer surfaces (Tanaka & Sackmann,

2005). A number of natural and synthetic polymers are currently being employed as tissue scaffolds. Biodegradable synthetic polymers, such as poly(glycolic acid) (PGA), polyethylene glycol (PEG), poly(ethylene oxide) (PEO), polycaprolactone (PCL), poly(lactic acid) (PLA), polylactones, polyanhydrides, polyorthoester and polyurethanes have been used in a number of clinical applications (Behravesch et al., 1999). Thus, it is proved that polymers are essential for tissue engineering scaffolds.

Among the families of synthetic polymers, the polyesters have been attractive for these applications because of their easy degradation by hydrolysis of ester linkage, degradation products being resorbed through the metabolic pathways in some cases, and the potential to tailor the structure to modulate degradation kinetics. Polyesters have also been considered for development of tissue engineering scaffolds, particularly for bone tissue engineering. Poly-L-Lactide acid (PLLA) is also popular synthetic polymers in biomedical field.

4.1 Biodegradable polymers

The term “biodegradable polymers” denotes water insoluble polymers which, by means of a chemical reaction in the body, are converted slowly to water soluble materials. The polymers can have a side chain that undergoes hydrolysis in the body to produce hydroxyl, carboxyl or other hydrating groups. These groups make the polymer fragments and degradation products water soluble (Dunn, 1991). Another approach is to crosslink a water soluble polymer with a hydrolysable cross-linking agent. Once crosslinked, the polymer is insoluble. When placed in the body, the crosslinking group is hydrolyzed or degraded to give a water soluble polymer. Water insoluble polymers which contain hydrolysable functional groups directly in the polymer chain is degraded to shorter and shorter chain segments which eventually become water soluble. The main benefit of the latter group of polymer is that polymer will have good mechanical properties. Table 2 lists some examples of these biodegradable polymers.

Poly(lactic acid)	Polyorthoesters
Poly(glycolic acid)	Polycarbonates
Poly(glycolic acid)	Polyanhydrides
Polycaprolactone	Polyphosphate esters
Poly(hydroxybutyrate)	Polyphosphazenes

Table 2. Examples of biodegradable polymers

4.1.1 Polyethers

Poly(ethylene oxide) (PEO) and PEG have the same polymer structure made of different monomers; one is made from ring opening of ethylene oxide and one from the condensation of ethylene glycol, respectively. PEG's major attractiveness for seeding is that it does not present specific receptors for cell attachment. PEG has been approved by the FDA for several medical applications due to its biocompatibility and low toxicity. PEG has been extensively used as excipient in pharmaceutical formulation for oral and injectable administration to stabilize proteins by chemical conjugation of PEG, surface modification of biomaterials and induction of cell membrane fusion, and UV polymerization of the precursor that consists of PEG with acrylate terminal at each end in the presence of α -hydroxy acids. Star-shaped PEG has been cross-linked by interaction with liver cells (Maher et al., 2009a, 2009b).

4.1.2 Polyesters

Polyesters are synthesized by condensation polymerization of dicarboxylic acids. Polyhydroxybutyrate and polyhydroxyvalerate are developed by Imperial Chemical Industries (ICI) from a fermentation process of PCL. The homopolymers in these series are hydrophobic and crystalline in structure, and therefore, they have long degradation times in vivo (1-2 years). However, copolymerization (e.g. PCL-based) has led to materials to have relatively shorter degradation time because of changes in crystallinity and hydrophobicity of these polymers (Chaudhary et al. 1997).

Polyesters can also be formulated by stepwise polymerization and ring opening polymerization. One of the most versatile and widely used synthesized polymers is aliphatic polyesters prepared from lactic and glycolic acids. These polymers were first utilized as sutures and orthopaedic plates and nails, and their biocompatibility and biodegradability are well known. Moreover, the commercial availability of these polymers along with favourable biodegradation rates has made these polymers as the first choice of medical devices. The applications are also found in controlled release of gene delivery and tissue engineering.

4.1.3 Copolymers

Combinations of biomaterials also provide better characteristics than a single biomaterial. For example, the composite of poly(L-lactic acid)/ β -tricalcium phosphate (PLLA /TCP) have better combination of properties as a scaffold material. The biodegradation rate of PLLA is too low to match the tissue regeneration process after implantation (Chuenjitkuntaworn et al.). The acidic degradation products of PLLA, such as lactic acid tend to cause aseptic inflammation in tissue (Moroni et al., 2006). On the other hand, TCP has a higher biodegradation rate; it has a hydrophilic surface; and its degradation products are often alkaline. But TCP has poor mechanical properties. According to the histological analysis of the implantation experimentation of PLLA/TCP composites manufactured by low-temperature deposition manufacturing (LDM) process, the scaffold were degraded in 24 weeks after implantation with no trace of aseptic inflammation found. As a scaffold material for bone TE, PLLA/TCP composite could be a better choice compared to the use of PLLA or TCP alone (Xiong et al., 2002).

PCL is commonly used biocompatible and biodegradable aliphatic polyester with low melting point and excellent solubility in most of the solvents. PCL is used in various biomedical applications such as urethral catheters, drug delivery systems, resorbable sutures etc., and has been proposed as a material for bone and cartilage tissue engineering (Barrows, 1986). When PCL is copolymerised with ethylene oxide (EO) or poly(ethylene glycol) (PEG) to prepare PCL-PEG-PEO block copolymers their hydrophilicity and biodegradability are improved, and thus they may find much wider applications. PEG presents outstanding properties, e.g. hydrophilicity, solubility in water and in organic solvents, nontoxicity, and absence of antigenicity and immunogenicity, which allow PEG to be used for many clinical applications. PEG of low molecular weight can be excreted through the kidney, so its biostability is not a problem. Recently, bioresorbable polyester-PEG diblock or triblock copolymers have been prepared by using a monohydroxy or α , ω -dihydroxy PEG as initiator for the polymerization of lactone monomers (Piao et al., 2003).

Various PEO based polymers have been reported and utilized especially in drug delivery. One interesting copolymer is a triblock copolymer of PEO and poly(propylene oxide) (PPO)

which is known under the trade name of Pluronic® or Poloxamers®, and is available in various lengths and compositions. These polymers form thermally reversible gels without any permanent cross-linking. Besides, PEO-PPO-PEO triblock copolymers can be designed to form gels at body temperature. A few PEO-PPO-PEO copolymers are in clinical use as surfactants and solubilizers in injectable formulations.

5. Scaffold fabrication techniques

5.1 Conventional techniques

Conventional fabrication techniques are defined as processes that build scaffolds having a bulk or porous (interconnected or non-interconnected) structure which lacks any long-range channelling microstructure. In contrast, solid free form fabrication uses layer manufacturing processes to form scaffolds directly from computer-generated models, thereby enabling the introduction of hollow or tubular structures in scaffolds. Additionally, solid freeform fabrication techniques enable the creation of external geometry of the scaffold with high precision. Conventional techniques are often used in scaffold fabrication for bone and cartilage tissue engineering. Commonly used scaffold fabrication techniques are listed in Table 3.

Scaffold fabrication Techniques	
Conventional	Rapid prototyping
Solvent casting/ particulate leaching	Stereolithography
Phase inversion/ particulate leaching	Fused deposition modeling
Fibre meshing/ bonding	Three dimensional printing
Melt moulding	Three dimensional plotting
Gas foaming	Selective laser sintering
Membrane lamination	Laminated object manufacturing
Hydrocarbon templating	Multiphase jet solidification
Freeze drying	
Emulsion freeze drying	
Solution casting	

Table 3. List of conventional and RP scaffold fabrication techniques

Gas foaming/high pressure processing technique is based on the CO₂ saturation of polymer disks through their exposure to high pressure CO₂. Prominent advantage of this method is the possibility of obtaining scaffolds with a high degree of porosity with a pore size range of 100 µm. However, low mechanical strength and poorly defined pore structure of the scaffold limit the widespread use of this technique.

A further method is based on a thermally induced phase separation (freeze-drying), which occurs when the temperature of a homogeneous polymer solution previously poured into a mould, is decreased. This technique allows the production of scaffolds consisting of natural and synthetic polymers. As the processing conditions are technically challenging and the developed scaffolds have low mechanical competence accompanied by reduced pore size, the application of this technique is also limited.

The varying success rates of the above-mentioned scaffold fabrication methods may be due to the extensive involvement of manual intervention, and the inconsistent and inflexible processing procedures.

5.2 Rapid Prototyping techniques

RP technology is launched in the market during late 1980s with the introduction of the stereolithography system by 3D Systems Inc (Holland & Tighe, 1992; Legault, 2008). RP also termed as “solid freeform fabrication” is a relatively new technology that generates a physical model directly from computer-aided design (CAD) data in a layer-by-layer manner. RP techniques have been identified and recognized to possess significant potentials for fabricating tissue engineering scaffold. RP has been used in the medical field primarily as a means of guiding surgical procedures using tactile models derived from patient computerized tomography (CT) data. The potential to intimately control the microstructure of porous channels and the overall macroscopic shape of the implants makes RP an ideal process for fabricating implant and tissue engineering scaffold as well. Direct fabrication of customized implants is promising in offering simpler and more rapid surgical implementations.

RP fabrication begins with the development of a 3D volumetric computer model of the desired part that can be derived from output data generated by surface digitizers or medical imaging systems (e. g. Computed Tomography or Magnetic Resonance Imaging etc.). The 3D architecture and geometry of porous microstructure determined by pore size, shape, interconnectivity, and anisotropy are the key design parameters. RP technique allows the fabrication of scaffolds with controlled pore network and with a custom made shape. The digital model is then mathematically sliced into thin layers having a constant thickness that is user-defined. Then layers of material representing the cross-sectional profiles of the desired part as obtained from the computer generated slices are formed by processing solid sheet, liquid or powder material feed stocks. The material layers are automatically and precisely stacked and fused on top of one another to create the desired physical part (Chua & Leong, 1997; Leong et al., 2003) (see Fig. 3). Furthermore, advances in in-vivo imaging, such as positron emission tomography, make it possible to provide a confined monitoring of the development and incorporation of the engineered tissues (Chua et al., 2009; Chua & Leong, 1997).

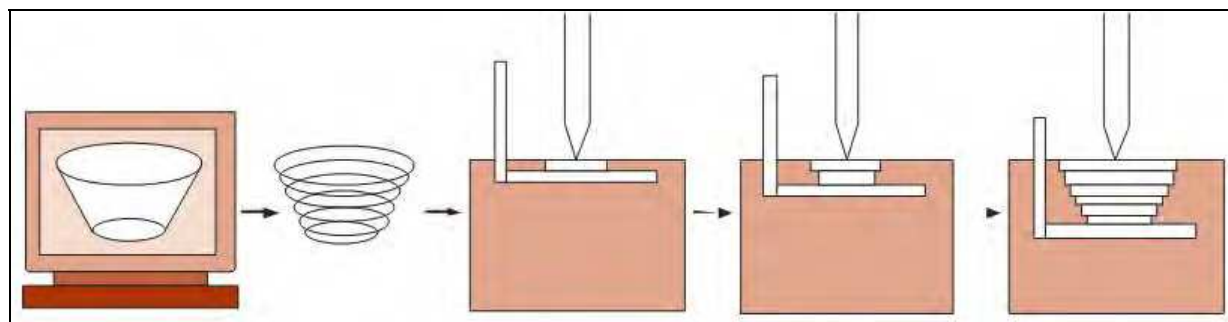


Fig. 3. RP fabrication: From CAD data to layer-by-layer construction (Yeong et al., 2004)

RP techniques are beneficial for tissue engineering scaffold fabrication due to their ability to address and overcome the problems of uncontrollable microstructure and the ability to manufacture complex 3D structures. These techniques have rigorous control over porosity, pore size, stiffness and permeability; the RP scaffolds are usually designed to have fully interconnected pore structure. This method is particularly useful for tissue engineering since it allows a very good reproducibility and the production of almost any kind of structure within the limitations of each technique used. It is possible to design a structure that mimics the natural tissue to be replaced (Daily, 2010). Such capabilities are highly advantageous since the

ideal scaffold should replicate the geometry and size of the patient's original anatomy and its internal micro-architecture. RP offers freedom of varying structural parameters to the non-variable bulk mechanical properties of the material used (Moroni et al., 2006). Each tissue and organ in the human body has their own unique geometry which varies in size among individuals. This fact undermines the applicability of most conventional fabrication techniques which are restricted to the fabrication of scaffold with highly simplified geometries.

Besides, RP techniques also allow the investigation of the effect of scaffold geometry on cell behaviour for further optimization of the scaffold design (Starly et al., 2006). Lacroix and Prendergast (2002) have introduced computational models to tissue regeneration as a predictive tool, and proposed a modified mechano-regulation theory based on the influence of morphologic parameters (pore shape, size, distribution and interconnectivity) and loading conditions (compression load and fluid perfusion) on the response of surface stimuli. Based on the selection of a regular microstructure and optimal inlet conditions, it is possible to predict the initial stimuli felt by the cell, in order to analyze and propose a scaffold design with specific function, such as bone or cartilage tissue differentiation.

However, not all RP methods are applicable for all polymeric materials for scaffold fabrication. For example, moulding methods are inappropriate for developing hydrogel scaffolds because, the scaffold cannot be removed without damaging both internal and external architecture (Mastrogiacomo et al., 2005). Porous hydrogel scaffolds are difficult to develop, especially when integrating tight interconnecting pores. There are very few reports on any RP technology producing scaffolds with consistent pore definition in the range of 200-400 μm , while also retaining a high accuracy of outside architecture (Maher et al., 2009a & 2009b). Hydrogel with low viscosities tend to be difficult to use when constructing scaffolds because of the long gelation time which results in the collapse of scaffolds due to their mechanical instability (Cunha et al., 2005). Fig. 4 presents the overview of RP technologies applied in processing various biomaterials for biomedical applications (Bergman & JI, 2008).

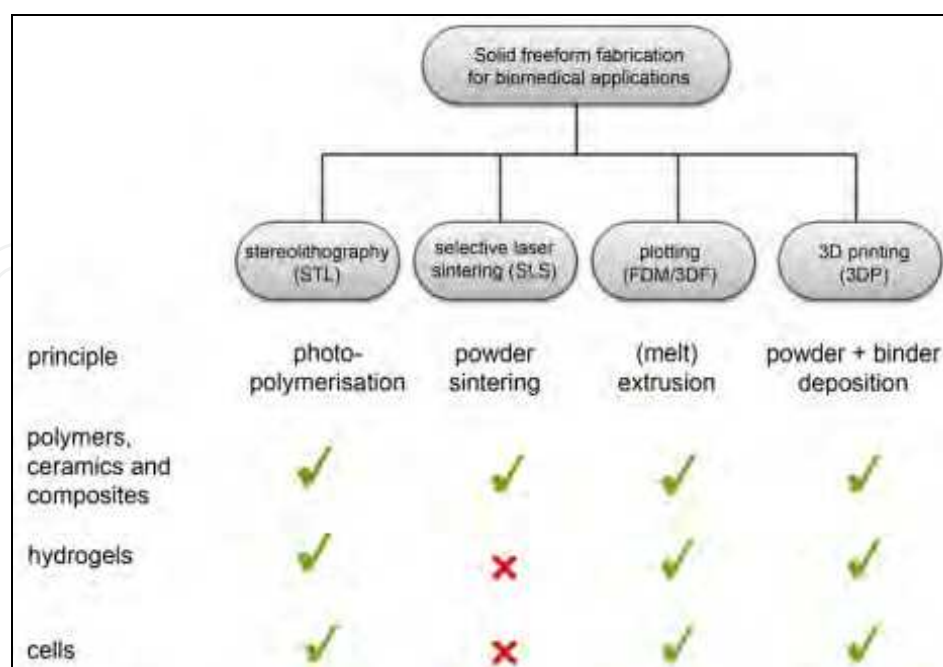


Fig. 4. Overview of RP technologies applied in processing various biomaterials for biomedical applications (Bergman & JI, 2008).

Although the application of RP technology for the production of tissue engineering scaffolds is still very much in the laboratories, the vast interest in RP technology for tissue engineering scaffold fabrication has been evidenced by the huge number of publications generated over the last 5 years. Research conducted with existing commercial and non-commercial RP systems has laid down a firm foundation in generating scaffolds with unprecedented quality, accuracy and reproducibility. Table 4 summarizes the advantages and limitations of various RP techniques.

Techniques	Advantages	Limitations
Sheet lamination e.g. Laminated object manufacturing (LOM)	No additional support is required	Materials trapped in small inner holes is impossible to be removed
Adhesion bonding e.g. 3-dimensional printing (3DP)	More materials choice; Low heat effect on raw powder	Materials trapped in small inner holes is difficult to be removed
Powder sintering e.g. selective laser sintering (SLS)	Relative higher part strength. More materials choice.	Material trapped in small inner holes is difficult to be removed; biodegradable materials may be degraded in the chamber
Photopolymerization Stereolithography (SLA)	Relative easy to remove support materials; relative easy to achieve small feature.	Limited by the development of photopolymerizable and biocompatible, biodegradable liquid polymer material
Droplet deposition e.g. fused deposition modeling (FDM)	No materials trapped in the scaffold easy to achieve, 100 μm scaffold features	Relative regular structure; anisotropy between XY and Z direction; High heat effect on raw material
Model maker	Easy to achieve ,100 μm or smaller scaffold feature	High heat effect on raw material; difficult to change materials without manufacturer's cooperation

Table 4. Summary of the advantages and limitations of various RP techniques.

To date, quite a number of RP techniques have been exploited for scaffold fabrication though most of the commercially available RP systems are designed to cater mainly for industrial engineering applications. The next section reports a study on the evaluation of the scaffolds developed by desktop robot based rapid prototyping (DRBRP) system.

6. Scaffolds developed by DRBRP system

6.1 Introduction

At present, solid freeform fabrication (SSF) is considered to be the best way to generate defined porous structures. SSF technology in combination with 3D imaging reconstructed based on CT and/or MRI data, is able to form high precision realistic models. We have

developed a SSF technique, called desktop robot based rapid prototyping (DRBRP) system (Hoque et al., 2005, 2008) in-house, which is capable of extruding biopolymer for freeform construction of 3D tissue engineering scaffold. The DRBRP system was tested through fabrication of various scaffolds with a number of polymers, like PCL, PCL-PEG and PCL-PEG-CL, and lay-down patterns. The 3D scaffold was modelled as per Fig. 5 that is composed of series scaffold architectures. Scanning electron microscopy (SEM), gas pycnometry, micro-computed tomography (micro-CT) and compression test were performed to characterize the morphology and mechanical properties of the resulting scaffolds. The cell response to the as-fabricated scaffolds was evaluated using rabbit smooth muscle cells (rSMCs). The cell morphology was investigated by light, scanning and confocal laser microscopy. Interconnected pores that allow cell growth to penetrate the 3D matrices are formed between the adjacent filaments.

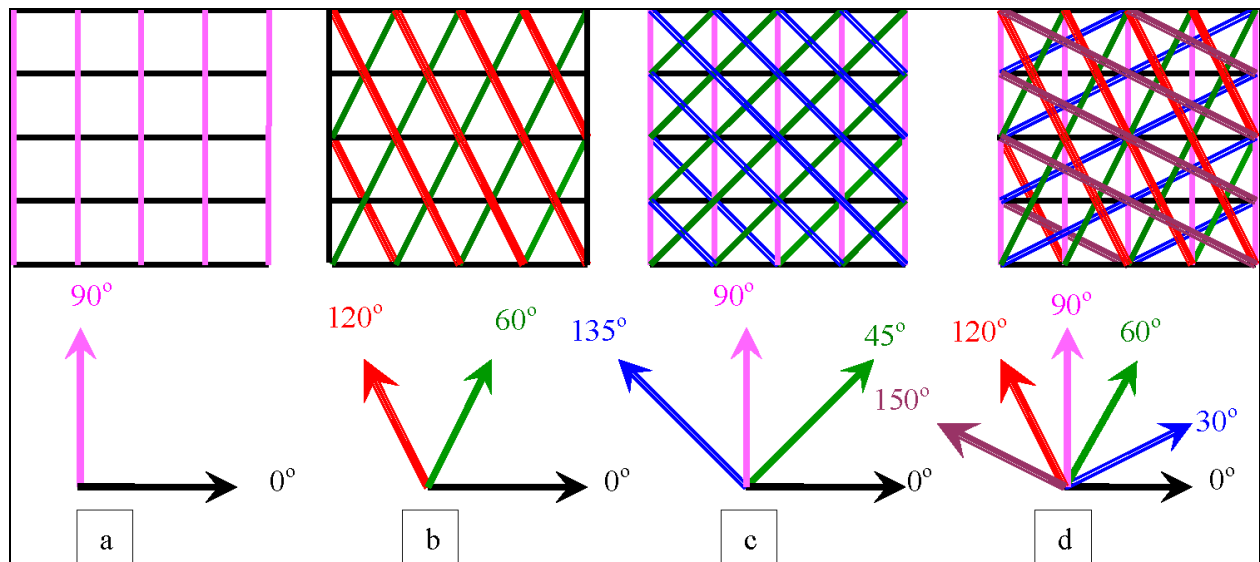


Fig. 5. Various lay-down patterns selected to process TE scaffolds. (a) 0/90°, (b) 0/60/120°, (c) 0/45/90/135° and (d) 0/30/60/90/120/150° (Hoque et al., 2005)

6.2 Manufacturing of scaffolds

The in-house built DRBRP system combined with a simple and user-friendly software code was used to manufacture 3D scaffolds. From a biomaterial point of view, this RP system is very versatile and is capable of extruding hot melts, solutions, pastes and dispersions of polymers as well as monomers and reactive oligomers. DRBRP system is considered to be one of the most convenient available extruding deposition fabrication techniques due to its user friendly operation conditions, fully utilizable polymer feed, and the ability to produce scaffolds without any binders. Besides, this process is very appropriate to produce scaffolds for hard tissue engineering (e.g. bone). The DRBRP system consists of a computer-guided desktop robot (Robokids, Sony) (see Fig. 6), metallic chamber which is heated by an electrical band heater, and a pneumatic dispenser. The dispenser itself is consisted of an air filter, regulator, lubricator, a solenoid valve and a nozzle. The DRBRP system allows biopolymer to be fed virtually in any form (e.g. pellet, lump, powder etc.) for processing into 3D scaffold. Software used in the developed DRBRP system was made up of a slicing and dispensing program, allowing users to generate geometrical data of 3D scaffolds

through user-friendly interfaces. The geometrical data can be automatically generated by using the slicing program written in-house. The 3D model can be segmented in stereolithography (.stl) file format into 2D layers by specifying the required control parameters.

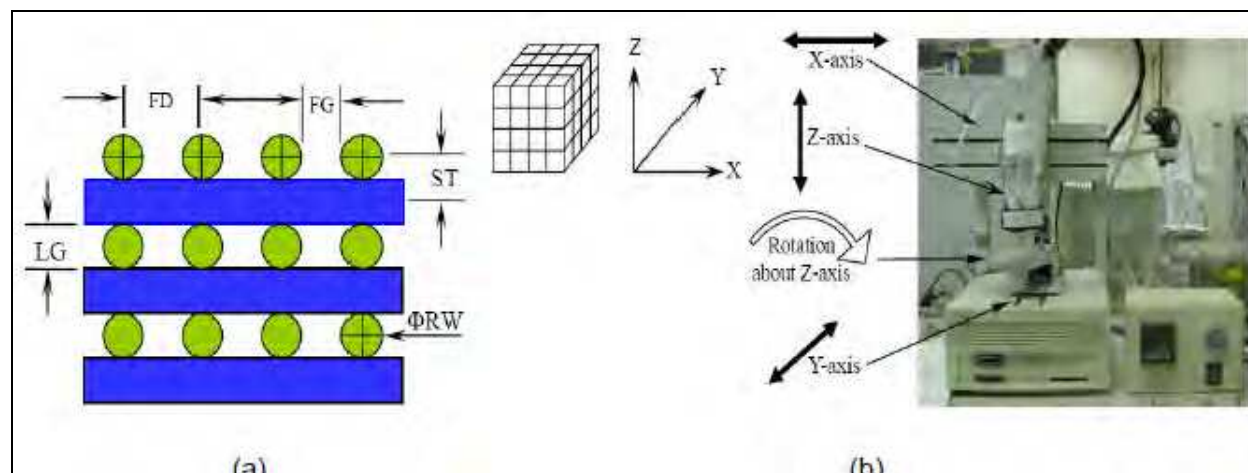


Fig. 6. (a) Model of lay-down pattern (0/90) viewed in cross section. Road width (RW): diameter of the filament, filament distance (FD): the centre-to-centre horizontal distance between two consecutive filaments in the same layer, fill gap (FG): edge-to-edge horizontal distance between adjacent filaments, layer gap (LG): edge-to-edge vertical distance between layers of the same filament alignment, slice thickness (ST): the vertical distance between the filament centre of adjacent layers. (b) DRBRP system demonstrating the coordinate directions of scaffold fabrication (Hoque et al., 2008).

The thermoplastic polymers were melted in the stainless steel chamber of the DRBRP system by electrical heating and extruded out by means of compressed air pressure through a mini nozzle to build scaffold. The process of deposition in each layer starts with formation of a “road” of molten material, called filament with user-defined width and thickness as presented in Fig. 6. The scaffold was built in an additive manner: line-by-line to form a 2D layer and layer-by-layer to form the 3D structure. Once a layer was completed, the dispenser moved up vertically in the Z-direction by a small displacement equivalent to the specified ST. To investigate the processing feasibility of the selected polymers, the lay-down pattern, nozzle size, and FD were selected as 0/90°, 500 μm , and 1.5mm, respectively. The liquefier temperature (the temperature used to keep the polymer molten), extrusion pressure (the pressure by which the polymer melt was extruded), and deposition speed (the speed at which the molten polymer was drawn) were set at 90°C, 4.0 bars, and 300mm/min, respectively, while the ambient temperature was maintained at 25±2°C. It was hypothesized that all three polymers (PCL, PCL-PEG, and PCL-PEG-PCL) have same rheological properties as they have very close melting temperatures (~65°C). Hence, for convenience, the same process conditions were applied to all tested polymers. The influences of processing parameters were studied by fabricating scaffolds with a single lay-down pattern 0/90° using two polymers (PCL and PCL-PEG) and employing three values of each parameter. For example, liquefier temperatures of 80°C, 90°C, and 100°C, extrusion pressures of 3.0, 4.0, and 5.0 bars, and deposition speeds of 240, 300, and 360mm/min.

During the fabrication, one parameter was varied iteratively, while the other two were remained constant. For cell culture studies, the scaffolds were fabricated with three lay-down patterns (0/30°C, 0/60°C, and 0/90°C) and two polymers (PCL and PCL-PEG) applying liquefier temperature, extrusion pressure, and deposition speed of 90°C, 4.0 bars, and 300mm/min, respectively. In all cases, the bulk scaffolds (50.0 x 50.0 x 5.0mm) were built on a flat plastic platform and removed upon fabrication, and cut into smaller blocks (e.g., 6.0 x 6.0 x 5.0mm) with an ultra-sharp blade for further testing.

6.3 Characterization of scaffolds

6.3.1 Scanning electron microscopy

The scaffold morphologies were observed by scanning electron microscope (SEM) (JSM-5800LV; Jeol USA, Peabody, MA) at 15 kV and a current of 60–90 mA. We studied the influences of process parameters on the scaffolds' porous characteristics. The top and cross-sectional views of scaffolds were obtained using a SEM for the morphological study. Briefly, scaffolds were fixed to a stub with carbon paint and coated with gold using a JEOL fine sputter coater (JFC-1200) for 60 s at 10 mA then viewed under the SEM. The pore dimensions were measured from the SEM images. The pore dimensions in different directions of fabrication process are not essentially the same. In the X- or Y-direction, the pore width is formed in between the intercrossing of filaments and hence is defined by the difference between FD and RW. Likewise, the pore height in the Z-direction is formed from void produced by the stacking of filament layers, and thus their size is regulated by the layer gap (LG).

The scaffolds fabricated with PCL, PCL-PEG, and PCL-PEG-PCL polymers exhibited homogeneous and consistent deposition of microfilaments with highly reproducible spatial arrangement of pores and channels when viewed in the Z-direction of the fabrication process (see Fig. 7). The cross-sectional views of the SEM images revealed the complete interconnectivity and integrity of the 3D porous scaffolds. It was also observed that the filaments fused evenly at the junctions, which resisted interlayer delamination. The reproducibility and regularity of the scaffold's pore networks were comparable to scaffolds fabricated by some other techniques, such as FDM, 3D fibre deposition, and precision extruding deposition. The SEM analysis (see Figs. 8-10) also dictates that the changes in process parameters significantly affected the scaffold morphologies.

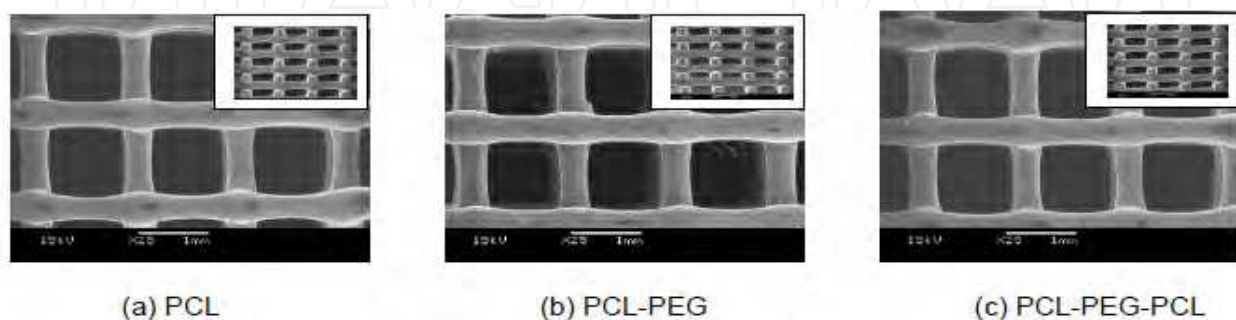


Fig. 7. SEM images of (a) PCL, (b) PCL-PEG, and (c) PCL-PEG-PCL scaffolds fabricated with three different polymers (pattern, 0=90; nozzle size, 500 μ m; FD, 1.5 mm). Plan view; insets, cross-sectional view (magnification, x25). SEM, scanning electron microscopy (Hoque et al., 2008).

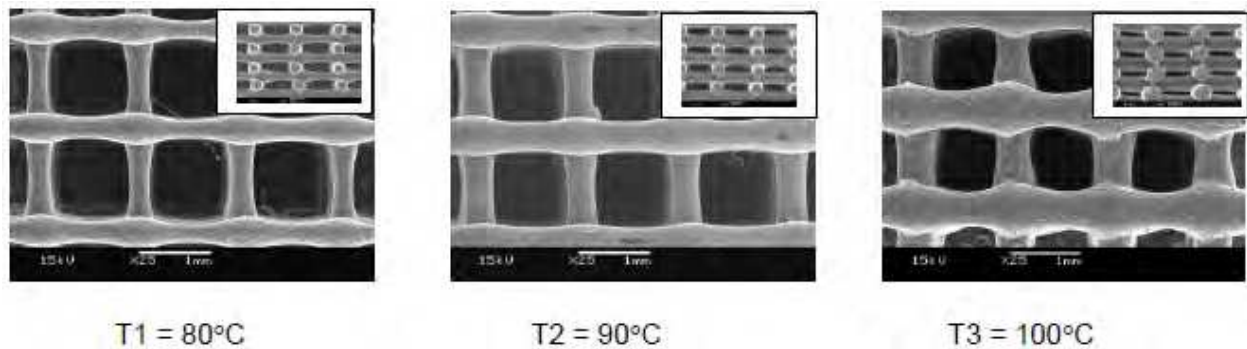


Fig. 8. SEM images of PCL-PEG scaffolds demonstrating the influence of liquefier temperature on their morphologies that indicates the gradual increase of filament diameter with the increase of liquefier temperature (nozzle size: 500 μm ; FD: 1.5mm). Big picture: plan view; small window: cross-sectional view (magnification $\times 25$) (Hoque et al., 2008).

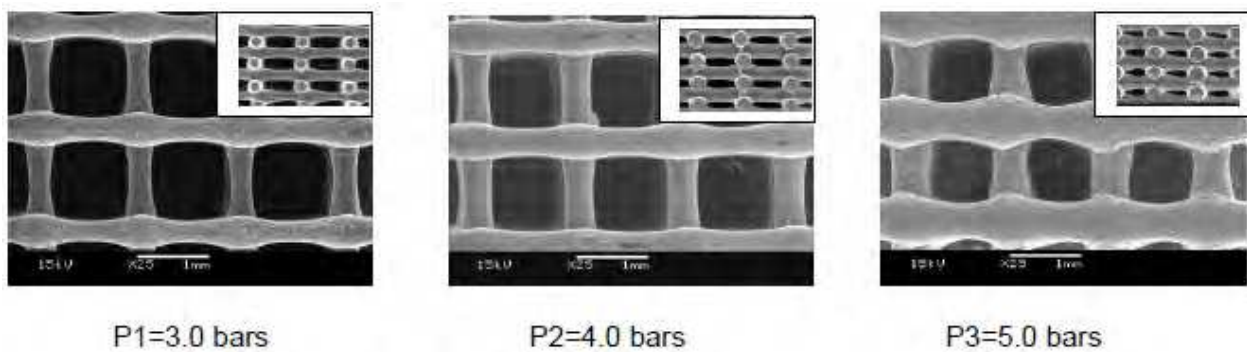


Fig. 9. SEM images of PCL-PEG scaffolds demonstrating the influence of extrusion pressure on their morphologies that indicates the gradual increase of filament diameter with the increase of extrusion pressure (nozzle size: 500 μm ; FD: 1.5mm) (Hoque et al., 2008).

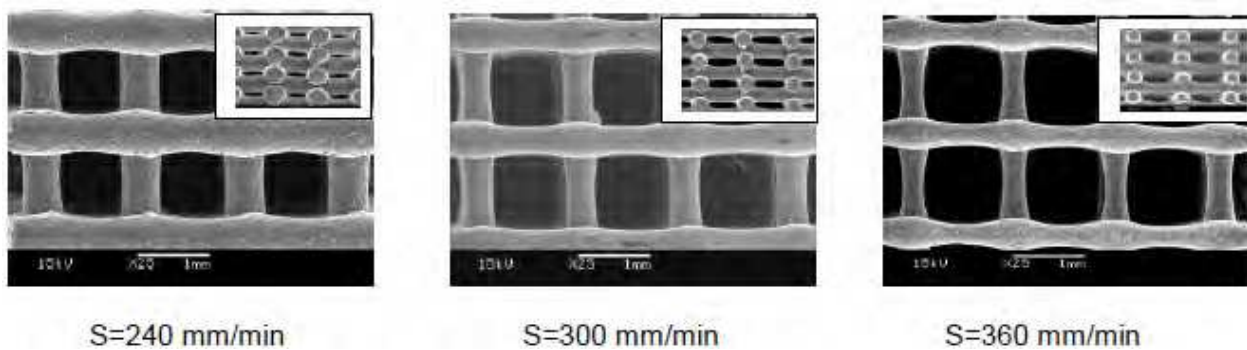


Fig. 10. SEM images PCL-PEG scaffolds demonstrating the influence of deposition speed on their morphologies that indicated the gradual decrease of filament diameter with the increase of deposition speed (nozzle size: 500 μm ; FD: 1.5mm) (Hoque et al., 2008).

6.3.2 Porosity measurement

The porosity values of the scaffolds with different architectures were determined using the following equation:

$$P = [(V_a - V_t)/V_a] \times 100\% \quad (1)$$

where, V_a (mm^3) is the apparent volume calculated based on the geometry of each scaffold block and V_t (mm^3) is the true volume. The true volume of each scaffold specimen was measured by using a gas pycnometer (Ultrapycnometer 1000, Quantachrome, Boynton Beach, FL, USA) at 25°C in pure argon. The porosity values were also determined by Micro-computed Tomography (micro-CT) analysis.

6.3.3 Micro-computed tomography

The morphology and microstructural formability of fabricated scaffolds were investigated using a Skyscan 1072 micro-CT desktop scanner (Skyscan, Kontich, Belgium). The micro-CT was set at 19 mm resolution. Two-dimensional analyses and 3D reconstructions of core regions of the samples were performed, which enabled calculation of the porosity, interconnectivity, and surface-to-volume ratio of the scaffolds.

The influences of process parameters on scaffold's porous characteristics were almost identical for both polymers namely, PCL and PCL-PEG. Likewise, the porosity values measured by ultrapycometer and micro-CT methods were found to be quite similar. Therefore, for simplicity, the porous characteristics refer to that of PCL-PEG scaffolds, and the porosities refer to the values measured by micro-CT method throughout the text, unless mentioned otherwise.

6.4 Influences of process parameters

The deposition tests discussed here were conducted to assess the effects of three main process parameters on the scaffold design of the resulting track and their suitability for layer deposition. In each test, one parameter was varied whilst the remaining parameters were set at a predetermined value. Table 5 lists the testing range and fixed value of each parameter.

Process parameter	Parameter range
Liquefier temperature	80°C - 100°C
Extrusion pressure	3 - 5 bars
Deposition speed	240 - 360mm/min

Table 5. Process parameter ranges investigated during deposition trials

Liquefier Temperature: The increase in liquefier temperature resulted in an increase of RW and thus decreased the pore size and porosity at a specific extrusion pressure and deposition speed. The fluidity of the polymer melt increased with increasing temperature, and it rendered faster and excessive dispensing of the polymer melt. The morphological changes due to change of liquefier temperature are presented in Table 6. An increase of temperature from 80°C to 100°C resulted in an increase of RW from 375 ± 45 to 620 ± 45 μm , which corresponded to a decrease of pore width in X- or Y-direction from 1125 ± 90 to 880 ± 90 μm , pore height in Z-direction from 330 ± 38 to 120 ± 20 μm , and porosity from 72% to 48%, respectively. The influence of liquefier temperature was also evidenced by the morphological change as observed in Fig.8.

Extrusion Pressure: Similar to liquefier temperature, increasing the extrusion pressure led to the increase of RW and thus decreased the pore size and porosity at a given condition of temperature and speed as presented in Table 7. An increase of pressure from 3 to 5 bars resulted in an increase of RW from 380 ± 50 to 623 ± 45 μm and a decrease of pore width from 1120 ± 100 to 877 ± 90 μm , pore height from 325 ± 35 to 118 ± 18 μm , and, consequently,

porosity from 73% to 47%. The influence of extrusion pressure was also evidenced by the morphological change as observed in Fig.9.

Temperature (°C)	RW (µm)	Pore Width (µm)	Pore Height (µm)	Porosity (%)	S/V Ratio (mm ² /mm ³)	Inter-Connectivity (%)
80	375±45	1125±90	330±38	72±2.88	12.10	100
90	500±25	1000±50	230±30	65±2.56	10.92	100
100	620±45	880±90	120±20	48±1.92	8.07	100

Table 6. Morphological changes due to change of liquefier temperature, while extrusion pressure and deposition speed remained constant at 4 bar and 300 mm/min, respectively. (Hoque et al., 2008)

Pressure (bars)	RW (µm)	Pore Width (µm)	Pore Height (µm)	Porosity (%)	S/V Ratio (mm ² /mm ³)	Inter-Connectivity (%)
3.0	380±50	1120±100	325±35	73±2.92	12.27	100
4.0	500±25	1000±50	230±30	66±2.64	11.09	100
5.0	623±45	877±90	118±18	47±1.88	7.90	100

Table 7. Morphological change due to change of extrusion pressure while liquefier temperature and deposition speed remained fixed at 90°C and 300 mm/min, respectively. (Hoque et al., 2008)

Deposition Speed: Unlike liquefier temperature and extrusion pressure, increase of deposition speed rendered lower polymer flow per travel distance, and thus decreased RW and increased pore size and porosity. In such case, the polymer melt is dispensed out at a specific flow rate under certain conditions, whereas the nozzle draws the melt faster at high deposition speed. This can be explained using the following flow rate equation:

$$A_i S_i = A_f S_f \tag{2}$$

where, A is the cross-sectional area of polymer melt that in turn is equivalent to the filament diameter, and S is the deposition speed. Subscripts 'i' and 'f' refer to initial and final values. If S increases, the filament diameter must decrease to maintain specific flow rate. The increase of deposition speed from 240 to 360mm/min resulted in a decrease of RW from 615 ±40 to 377 ±48 µm that accordingly increased the pore width from 885 ±80 to 1123 ±100 µm, pore height from 125 ±22 to 340 ±30 µm, and porosity from 45% to 75%, respectively, as presented in Table 8. The influence of deposition speed was also evidenced by the morphological change as observed in Fig.8.

6.5 Mechanical properties of scaffolds

For each envisioned application, successful tissue engineering scaffolds constructs will have certain minimum requirements for biological, biochemical and physical properties. For example, scaffold is required to provide sufficient initial mechanical strength and stiffness as substitute for the mechanical function of the diseased or damaged tissue to be repaired or regenerated.

Speed (mm/min)	RW (μm)	Pore Width (μm)	Pore Height (μm)	Porosity (%)	S/V Ratio (mm^2/mm^3)	Inter-Connectivity (%)
240	615 \pm 40	885 \pm 80	125 \pm 22	45 \pm 1.80	7.56	100
300	500 \pm 25	1000 \pm 50	230 \pm 30	66 \pm 2.64	11.09	100
360	377 \pm 48	1123 \pm 100	340 \pm 30	75 \pm 3.0	12.60	100

Table 8. Morphological change due to change of deposition speed while liquefier temperature and extrusion pressure remained fixed at 90°C and 300 mm/min, respectively. (Hoque et al., 2008)

In this study, the mechanical behaviour of the scaffold was investigated via uniaxial compression tests. Compression tests were carried out to evaluate compression behaviour of scaffolds and further to investigate the influences of process parameters on their mechanical properties. For each structural configuration, five samples (6.0 x 6.0 x 5.0mm) were tested. They were tested using a uniaxial testing machine (Instron 4502, Norwood, MA) and a 1 kN load-cell (Canton, Norwood, MA) adopting the guidelines for compression testing of acrylic bone cement set in ASTM F451-99a. This is the latest edition of the standard currently used by a number of research groups to characterize the mechanical properties of bioresorbable scaffolds of similar geometry. The specimens were compressed in Z-direction of fabrication process at a crosshead speed of 1 mm/min between two steel plates up to a strain level of 60%. The modulus of elasticity, E was calculated as the slope of initial linear portion of the stress-strain curve neglecting any toe region formed due to the initial settling of the specimen. Compressive strength at yield, σ_y was defined as the intersection of the stress-strain curve with the modulus slope at an offset of 1.0% strain. A Student's t-test was performed in comparing mean values from all independent sample groups using a Minitab statistics software version 12.2 (Minitab, State College, PA) and a significance level of 0.05.

As compression strain increased, the 3D pores of the scaffolds were crushed and underwent a densification process. When the rods and struts were crushed, the scaffold became stiffer and the stress level rised quickly as demonstrated by Fig. 11. Therefore, stress-strain curves typically followed three distinct regions: (i) a linear elastic region, (ii) a plateau of roughly constant stress, and (iii) a final region of steeply rising stress. When the scaffolds were compressed in Z-direction of fabrication process it was the filament junctions of adjacent layers that mainly supported the applied load at the beginning. In this case, the initial linear elastic deformation involved significant shear deformation of the filament joints. On further compression, the linear elastic regime was truncated by sliding of filament layers, which also manifested as a plateau of constant stress on the stress-strain curve. The final failure occurred when the filaments of adjacent layers were crushed. To strengthen the scaffold structure, a large number of filament joints would be expected. The strengthening effect can also be dependent on the bond strength, (i.e. the perfection of fusion) between filaments at their joints, which in turn is dependent on the design and process parameters of the fabrication technique.

As the process parameters had direct influences on RW and in turn on porosity, they influenced the mechanical properties like modulus of elasticity, yield strength, and yield strain. The modulus of elasticity E (MPa), 1% offset yield strength, σ_y (MPa), and yield strain (%) values calculated from the stress-strain curves are presented in Tables 9-11 as functions

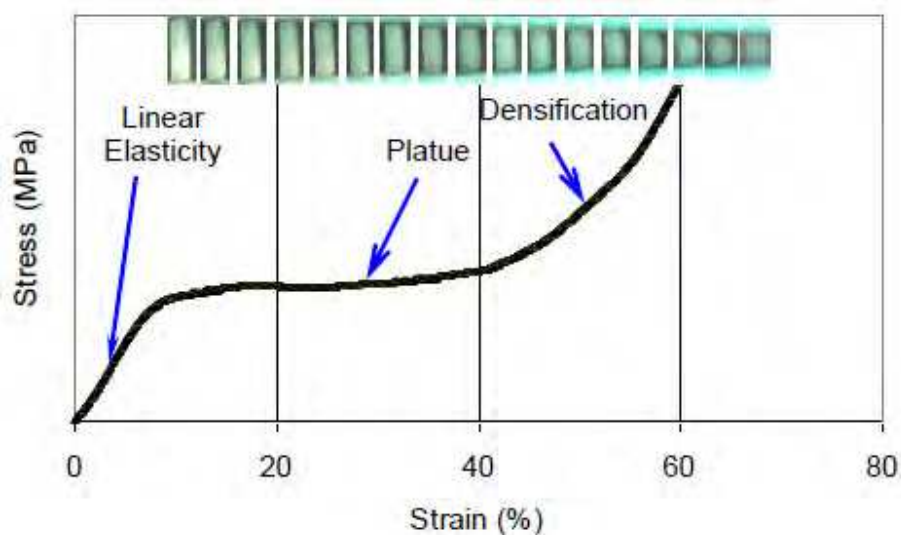


Fig. 11. Typical stress-strain curve of porous scaffold under compression showing linear elastic, plateau and densification regimes (Hoque et al., 2008)

of process parameters. Statistical analysis confirmed ($p < 0.05$) that for both PCL and PCL-PEG, increasing liquefier temperature and extrusion pressure resulted in thickening of extruded filaments (see Figs. 8 and 9) and decrease of porosity (Tables 6 and 7) with increased modulus of elasticity and yield strength (Tables 9 and 10). Unlikely, increase of deposition speed caused narrowing of filaments (see Fig. 10), and consequently, increased the porosity (Table 8) and decreased the modulus of elasticity and yield strength (Table 11). Similar trends were observed by Moroni et al. (2006) when changing the filament deposition speed.

Parameter	PCL			PCL-PEG		
	Elastic Modulus (MPa)	Yield Strength (MPa)	Yield Strain %	Elastic Modulus (MPa)	Yield Strength (MPa)	Yield Strain %
Temp (°C)						
80	29.31±1.17	2.26±0.09	2.87±0.11	25.05±1.00	1.9±0.07	2.45±0.09
90	36.08±1.44	2.79±0.31	3.59±0.14	30.83±1.23	2.2±0.08	3.06±0.12
100	53.6±2.14	4.14±0.16	5.33±0.21	45.8±1.83	4±0.16	4.6±0.18

Table 9. Influence of liquefier temperature on mechanical properties (Modulus of elasticity, yield strength and yield strain) of PCL and PCL-PEG scaffolds (Hoque et al., 2008)

Parameter	PCL			PCL-PEG		
	Elastic Modulus (MPa)	Yield Strength (MPa)	Yield Strain %	Elastic Modulus (MPa)	Yield Strength (MPa)	Yield Strain %
Pressure (bar)						
3	27.83±1.11	2.15±0.08	2.87±0.11	23.78±0.95	1.9±0.07	2.36±0.09
4	34.87±1.39	2.69±0.10	3.5±0.14	29.8±1.19	2.3±0.09	2.98±0.11
5	54.63±2.18	4.22±0.16	5.51±0.22	46.68±1.89	3.6±0.14	4.64±0.18

Table 10. Influence of extrusion pressure on mechanical properties (Modulus of elasticity, yield strength and yield strain) of PCL and PCL-PEG scaffolds (Hoque et al., 2008)

Parameter	PCL			PCL-PEG		
	Elastic Modulus (MPa)	Yield Strength (MPa)	Yield Strain %	Elastic Modulus (MPa)	Yield Strength (MPa)	Yield Strain %
240	59.31±2.37	4.58±0.18	5.64±0.22	50.68±2.02	3±0.12	4.81±0.19
300	37.47±1.49	2.9±0.11	3.49±0.13	32.02±1.28	2.47±0.09	3±0.12
360	27.44±1.09	2.12±0.08	2.56±0.10	23.45±0.93	1.81±0.07	2.19±0.08

Table 11. Influence of dispensing speed on mechanical properties (Modulus of elasticity, yield strength and yield strain) of PCL and PCL-PEG scaffolds (Hoque et al., 2008)

6.6 Cell culture study

Rabbit Smooth Muscle Cells (rSMC) were used to investigate the influences of polymer nature and scaffold architecture on cell performance in terms of cell attachment and proliferation on scaffolds. Two polymers (PCL and PCL-PEG) and three lay-down patterns (0/30, 0/60, and 0/90) were investigated.

6.6.1 Cell harvesting

These cells were obtained from the corpus cavernosa smooth muscle of the penis of a male New Zealand White Rabbit. The rabbit was routinely maintained under general anaesthesia by intubation with isoflurane. The local area was cleaned with iodine solution and alcohol, and was opened in layers until the cavernosal cavity was reached. About 1–2 mm of the corpus cavernosa smooth muscle tissue was biopsied, and the wound was closed in layers. The explants were finely minced and plated in a tissue culture flask containing low glucose Dulbecco's modified Eagle's medium supplemented with 10% fetal bovine serum and 1% penicillin-streptomycin.

6.6.2 Cell seeding

Following scaffold fabrication, the rSMC (passage 5) were seeded onto PCL and PCL-PEG scaffolds of 6.0 x 6.0 x 5.0mm with three lay-down patterns in a 24-suspension-well plate. The seeding density was 0.6×10^6 in 60 μ L suspension volume per scaffold. The cell-loaded scaffolds were left untouched in a self-sterilizable incubator (WTB Binder, Tuttlingen, Germany) at 37°C in 5% CO₂, 95% air, and 99% relative humidity for 3 h to allow protein secretion and cell attachment. Following 3 h of incubation, each well was filled with 1 mL of culture medium to submerge the scaffolds fully and placed back in the incubator. In the next day, the seeding efficiency was measured by transferring the cell-loaded scaffolds in the new plate. Half of the medium was changed after every 2 days, and the culture was continued for the period of 3 weeks. Throughout the study the low glucose Dulbecco's modified Eagle's medium supplemented with 10% fetal bovine serum and 1% penicillin-streptomycin was used. Phase contrast light microscopy (Leica DM IRB, Wetzlar, Germany) was used to examine the cell morphology, intercellular connections, and extracellular matrix production every week for the entire culture period of 3 weeks.

6.6.3 Cell Morphology

The biocompatibility of scaffold in terms of cell viability was assessed by the fluorescent staining of cell nuclei using confocal laser microscopy (CLM). The distribution, ratio of viable to dead cells in the cell-scaffold constructs, and stained cells embedded into scaffolds

were observed under the CLM (Zeiss LSM510 META, Oberkochen, Germany) on weeks 1 and 3. Viable cells were stained green with the fluorescent dye, fluorescein diacetate (FDA; Molecular Probes, Eugene, Oregon), and dead cells were stained red with propidium iodide (PI, Molecular Probes). The laser emission and excitation wavelengths were set at 510–560 nm and 488 nm, respectively, for FDA, whereas for PI they were set at 560–600 nm and 543 nm, respectively. Depth projection images were constructed from up to 25 horizontal image sections through the constructs.

Similarly, the cell adhesion and their distribution into the scaffolds were studied by SEM. The cells were fixed by means of 3% glutaraldehyde. The scaffold cell constructs were mounted on a stub using double-sided carbon tape, and sputter coated with gold (JFC-1200; Jeol) for 60 sec at 10 mA before viewing under the SEM. Then, the cell morphology was observed on the SEM (JSM-5800LV; Jeol) under high vacuum with an accelerating voltage of 15 kV and at a working distance of about 2 cm.

The rSMCs started attaching onto both PCL and PCL-PEG scaffold surfaces with all three lay-down patterns (0/30, 0/60, and 0/90) after 2 h of seeding. The initial round cells adhered to the scaffolds, migrated, and developed an interconnected cell network using the rods and struts as templates for their proliferation. At week 1 in culture, the cells demonstrated distinct morphological changes, while spreading on the bars and struts of the scaffold surface as well as bridging the adjacent bars as observed by phase contrast light microscopy and CLM presented in Figs. 12 and 13. As indicated by the confocal images using the live/dead stain FDA-PI, most of the cells were viable after week 1.

The cells progressed to bridge the walls of the fully interconnected pore network via 3D extracellular matrix (ECM) production. From this point on, the cell-to-cell contact points, the ECM, and culture media acted as templates. In general, the cells started the 3D growth process at the junctions of the bars and struts.

After the cells had grown over the surfaces of the rods and struts, they proceeded to fill up the pores in a circular manner. From qualitative assessment, cellular attachment and proliferation appeared to be higher on the PCL-PEG scaffolds than on the PCL scaffolds. The

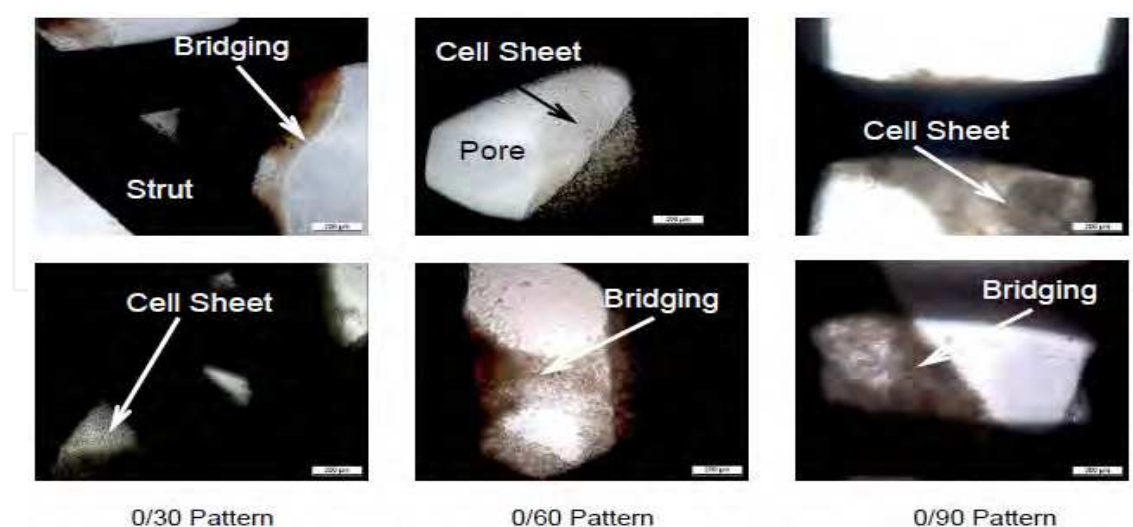


Fig. 12. Phase contrast light microscopy images of rSMCs attached to the PCL (top) and PCL-PEG (bottom) scaffolds with various lay-down patterns after 1 week in culture. Cell attachment and proliferation were increased on the PCL-PEG scaffolds compared to the PCL scaffolds (magnification, x10) (Hoque et al., 2008).

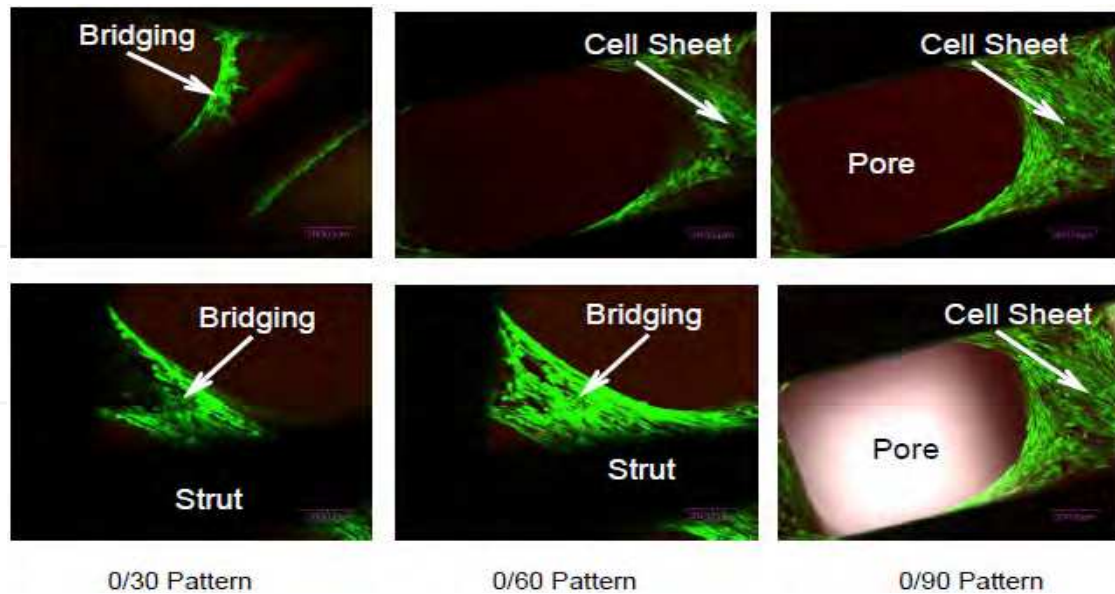


Fig. 13. CLM images of the statically seeded scaffolds after 1 week in culture. The scaffold architecture was partially covered by the cells demonstrating bridging the bars for both scaffold groups. Top row: PCL scaffolds; bottom row: PCL-PEG scaffolds (magnification, x10) (Hoque et al., 2008).

enhanced cell attachment on PCL-PEG surfaces observed by CLM could also have promoted cell proliferation. However, no significant differences in cell attachment and proliferation were observed among the scaffold patterns. Henceforth, phase contrast microscopy and CLM showed that after 3 weeks of culture, the entire architecture of both scaffold groups was filled with cells and extracellular matrix as demonstrated by Figs. 14 and 15.

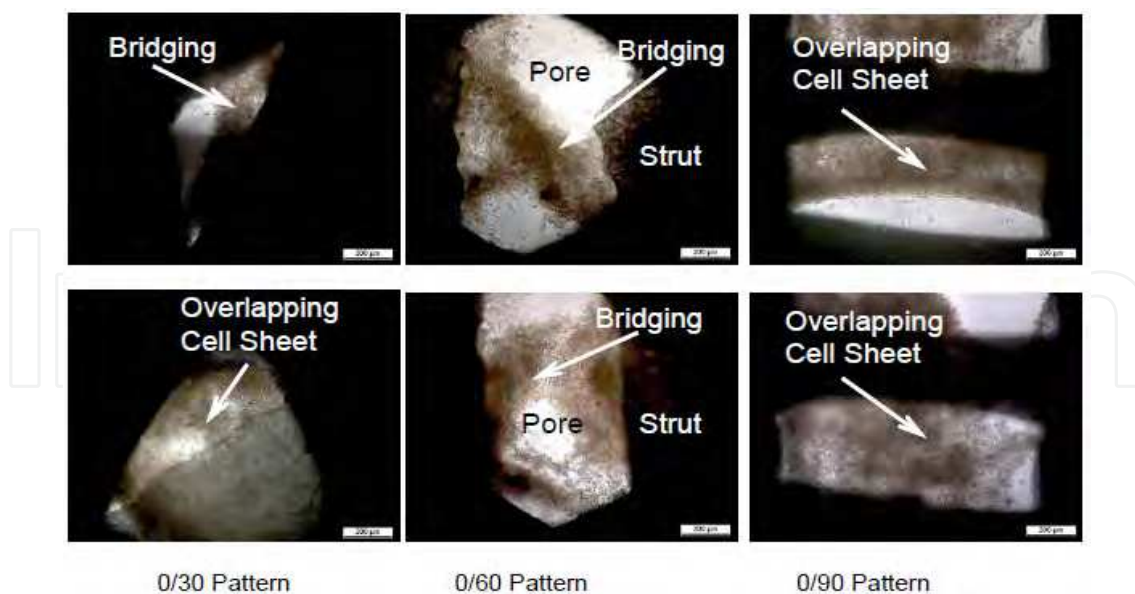


Fig. 14. Phase contrast light microscopy images of rSMCs attached to the PCL (top) and PCL-PEG scaffolds with various lay-down patterns after 3 weeks in culture. The cells continued to proliferate on all three patterns, leading to almost complete obliteration of the porous space of the scaffolds. Cells attachment and proliferation were increased on the PCL-PEG scaffolds compared to the PCL scaffolds (magnification, x10) (Hoque et al., 2008).

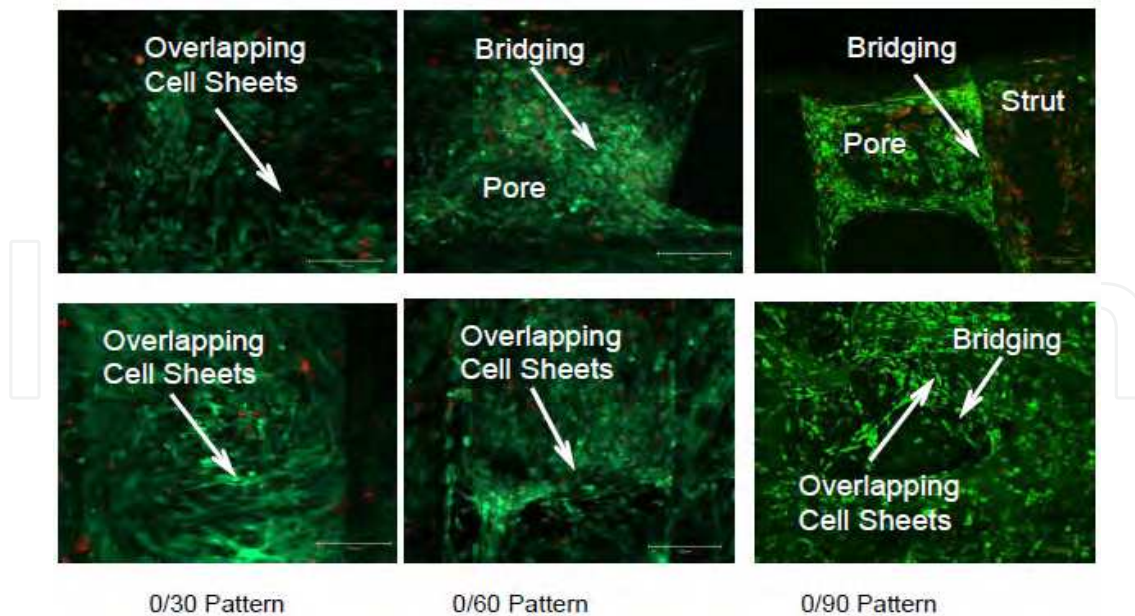


Fig. 15. CLM images of the statically seeded scaffolds after 3 weeks in culture. Almost entire scaffold architecture was covered by cells for both scaffold groups. However, the PCL-PEG scaffolds (bottom row) have denser cell ECM network than the PCL scaffolds (top row). The viable cells are stained with the green dye FDA, and nuclei of dead cells are indicated by red PI stain. The cell clusters in the pores show a high uptake of the FDA stain, indicating that the majority is alive. After 3 weeks of culture the FDA/PI staining still showed the viable cells inside the honeycomb scaffold architecture (magnification , x10) (Hoque et al., 2008).

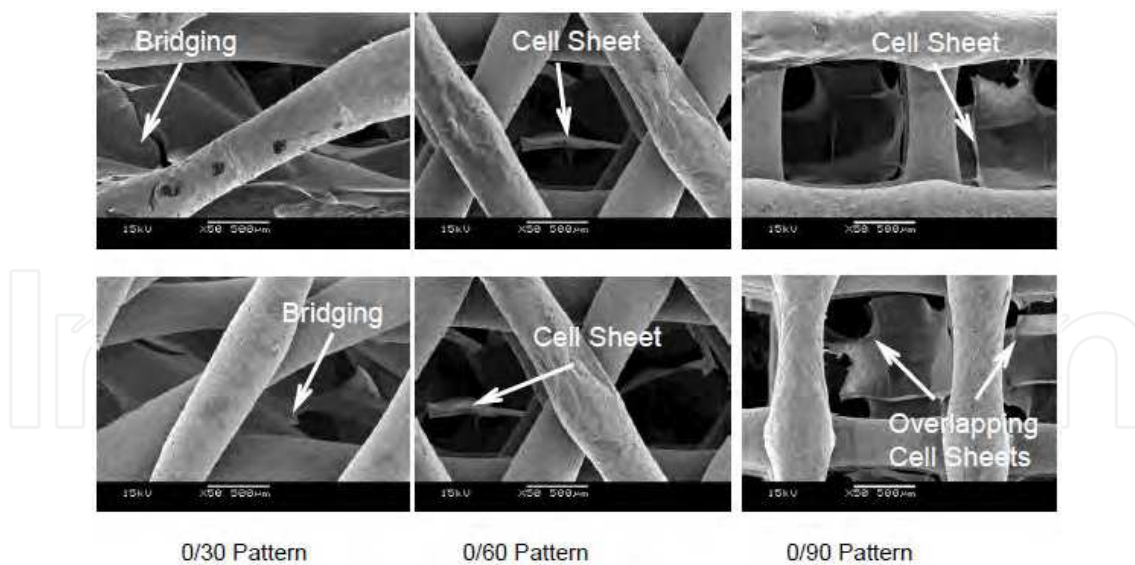


Fig. 16. SEM images of PCL (top) and PCL-PEG (bottom) scaffolds with cells after 3 weeks in culture. The entire surface scaffold architecture is covered with a dense cell-extracellular matrix. Cells bridging adjacent bars are present (magnification, x50) (Hoque et al., 2008).

Qualitative examination revealed that the major portion of the cells continued to remain viable as evidenced by the CLM images. The SEM images (see Fig. 16) showed that the overall scaffold architectures of both polymers were covered with a dense cell sheet though

not many cells were seen adhering onto the outer bars and struts of the scaffolds due to the fixation and specimen processing that resulted in the detachment of cells. However, based on the imaging data, no significant difference was detected among the scaffold patterns in respect to the proliferation pattern. It was thought to be because of the open pore structures of all three patterns that favoured the nutrients flow in and wastes flow out. Thus, the results of this study suggest that the PCL and PCL-PEG scaffold surfaces allowed attachment and colonization of rSMC on the struts and bars. Within a period of 3 weeks, the cells formed an interconnected cell-to-cell and cell-to-extracellular matrix network throughout the whole honeycomb-like scaffold structure. All microscopic images revealed increased cell density over time not only at the outer surfaces but also throughout the entire scaffold architecture. This finding carries importance in tissue engineering in which in vitro neo-tissue formation (cells + extracellular matrix) is desirable for achieving homogenous tissue formation in combination with vascularization in vivo.

6.6.4 DNA quantification

Specimens (n=3) harvested at weeks 1 and 3 were evaluated using the Pico®Green DNA quantification assay (Molecular Probes). Specimens were treated with 1 mL enzyme solution comprising of 0.25% trypsin (Hyclone, South Logan, UT), 0.1% collagenase I (Gibco, North Andover, MA), and 0.1% hyaluronidase (Sigma, St. Louis, MO) for 12 h at 37 ° C to break down extracellular matrix in order to obtain a homogenous cell suspension that was shortly spun. The aliquots of supernatant were then taken and their DNA contents were quantified using Pico®Green (Molecular Probes). Fluorescence of specimen well was measured with a plate reader (Genios®; Tecan Group, Maennedorf, Switzerland) at excitation and emission wavelengths of 485nm and 535nm, respectively. Fluorescence of reagent blank was subtracted from raw sample fluorescence recorded to give the corrected value. The amount of DNA was calculated by extrapolating a standard curve obtained by running the assay with a given DNA standard.

For the PCL and PCL-PEG scaffolds of three lay-down patterns seeded with rSMC, the DNA quantification results (see Fig. 17) demonstrated a higher amount of DNA in case of PCL-PEG copolymer scaffolds than in case of PCL homopolymer scaffolds ($p < 0.05$) over the whole time period of 3 weeks. The progress of culture period showed a significant increase in DNA quantity from week 1 to 3 time points for both scaffold groups, indicating an increase in cell proliferation. This was in agreement with the different microscopic image analyses, which revealed that after 3 weeks of culture the FDA/PI staining still showed the viable cells inside the honeycomb scaffold architecture.

No significant variation in DNA quantity was measured among the patterns of both groups of scaffolds. However, this can be applicable only when these studied scaffolds consisted of limited number of layers and large pores. The uninterrupted supply of nutrients into the fully interconnected open porous scaffolds might favour the continuous proliferation of the cells that resulted in increase in DNA quantity with the progress of culture period for both scaffold groups. The enhanced cell attachment on PCL-PEG scaffold surfaces observed by CLM and SEM could have promoted cell proliferation and thus resulted in higher DNA quantity than that for PCL scaffolds. The particular mechanism that promotes or blocks cell attachment, proliferation, and differentiation on PEG containing copolymer is not yet fully understood. However, it is known that PEG incorporation results in chemical and physical

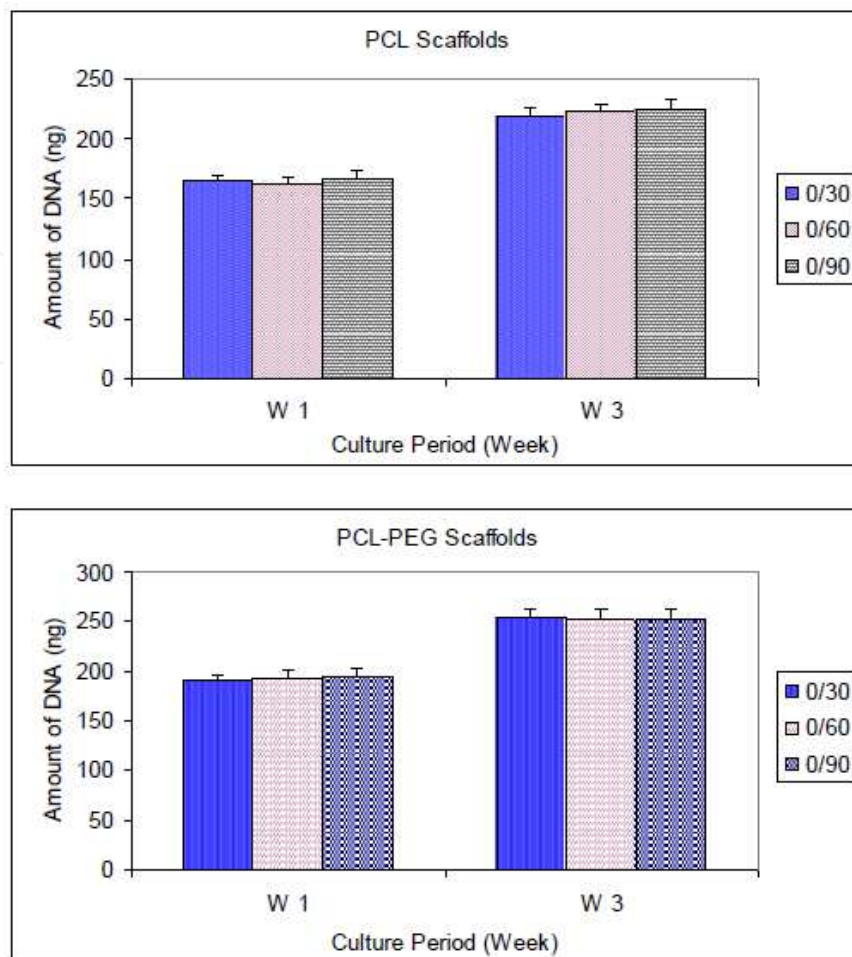


Fig. 17. PicoGreen results for PCL (top) and PCL-PEG (bottom) scaffolds with various lay-down patterns (Hoque et al., 2008).

changes on the copolymer surface. The PEG incorporation increases the overall hydrophilicity of the PCL-PEG copolymer surface as evidenced by reduced water contact angle (Hoque et. al., 2008). Similar cell response was reported by Huang and co-researchers (2010) who conducted in-vitro cell culture studies on PCL, PCL-PEG, and PCL-PEG- PCL scaffolds manufactured via solid freeform fabrication using primary human and rat bone marrow-derived stromal cells. Morphological characterization demonstrated the cell attachment, proliferation, and extracellular matrix production on the scaffold's surface as well as inside for all polymers. They also found that the copolymers showed better performance than the PCL homopolymer in their cell culture studies.

7. Conclusions

The DRBRP system successfully fabricated PCL, PCL-PEG and PCL-PEG-PCL 3D scaffolds with fully interconnected reproducible hierarchical pores. The process parameters intimately influenced the scaffolds' porous and mechanical characteristics. The PCL-based copolymers conserved the excellent thermal behaviour inherent to PCL, thus providing a

wide processing window for scaffold fabrication. Microscopic analyses showed adhesion, proliferation, and ECM production of the rSMCs on the surface as well as inside the structure of both scaffold groups (PCL and PCL-PEG). The completely interconnected and highly regular honeycomb-like pore morphology supported bridging of the pores via cell-to-cell contact as well as production of ECM. PCL-PEG copolymer scaffolds showed overall better performance in cell culture studies than the PCL homopolymer scaffolds that was reflected by the DNA quantification assay. However, the variation in lay-down pattern did not significantly influence the cell culture performance.

8. References

- Badylak, S. F. (2007). The Extracellular Matrix as a Biologic Scaffold Material. *Biomaterials*, Vol. 28, No.25, pp. 3587-3593, ISSN 0142-9612
- Barrows, T. (1986). Degradable Implant Materials: A Review of Synthetic Absorbable Polymers and their Applications. *Clinical Materials*, Vol. 1, No. 4, pp. 233-257, ISSN 0267-6605
- Behravesh, E. ; Yasko, A. W. ; Engle, P. S. & Mikos, A. G. (1999). Synthetic Biodegradable Polymers for Orthopaedic Applications. *Clinical Orthopaedics & Related Research*, Vol. 367, pp. 118-129, ISSN 0009-921X
- Bergman, N. & Ji, W. (2008). Principles of Regenerative Medicine. *Histogenesis in Three-Dimensional Scaffolds*. San Diego, Academic Press, ISBN 978-0-12-369410-2
- Chaudhary, A. K., Lopez, J., Beckman, E. J. & Russell, A. J. (1997) Biocatalytic Solvent-Free Polymerization to Produce High Molecular Weight Polyesters. *Biotechnology Progress*, Vol.13, No.3, pp.318-325, ISSN 1520-6033
- Chua, C. K. , Sudarmadji, N. , Leong, K. F. , Chou, S. M. , Lim, A. S. C. and Firdaus, W. M. (2009) Process flow for designing functionally graded tissue engineering scaffolds. *4th International Conference on Advanced Research in Virtual and Rapid Prototyping Leiria*, Portugal, 6-10 October 2009
- Chua, C. K. & Leong, K. F. (1997). *Rapid Prototyping: Principles and Applications in Manufacturing*, Wiley, ISBN 978-0471190042, New York, USA.
- Chuenjitkuntaworn, B., Inrung, W., Damrongsri, D., Mekaapiruk, K., Supaphol, P. & Pavasant, P. (2010). Polycaprolactone/Hydroxyapatite Composite Scaffolds: Preparation, Characterization, and In Vitro and In Vivo Biological Responses of Human Primary Bone Cells. *Journal Of Biomedical Materials Research Part A*, Vol. 94a, No.1, pp. 241-251, ISSN 1549-3296
- Cunha, P. L. R. ; Castro, R. R. ; Rocha, F. A. C. ; De Paula, R. C. M. & Feitosa, J. P. A. (2005). Low Viscosity Hydrogel of Guar Gum: Preparation and Physicochemical Characterization. *International Journal of Biological Macromolecules*, Vol. 37, No.1-2, pp. 99-104, ISSN 0141-8130
- Daily, S. (2010). 3-D Scaffold Provides Clean, Biodegradable Structure for Stem Cell Growth. *Science News*. In : *Science Daily*. University of Washington. Feb. 3, 2010 Available from <http://www.sciencedaily.com/releases/2010/02/100202174743.htm>

- Dodson, M. V.; Mathison, B. A. & Mathison, B. D. (1990). Effects of Medium and Substratum on Ovine Satellite Cell Attachment, Proliferation and Differentiation In Vitro. *Cell Differentiation and Development*, Vol. 29, No. 1, pp. 59-66, ISSN 0922-3371
- Domingos, M.; Dinucci, D.; Cometa, S.; Alderighi, M.; Bártolo, P. J. & Chiellini, F. (2009). Polycaprolactone Scaffolds Fabricated via Bioextrusion for Tissue Engineering Applications. *International Journal of Biomaterials*, Vol. 2009, No.2009, pp. 1-9, ISSN 1687-8787
- Drury, J. L. & Mooney, D. J. (2003). Hydrogels for Tissue Engineering: Scaffold Design Variables and Applications. *Biomaterials*, Vol. 24, No.24, pp. 4337-4351, ISSN 0142-9612
- Dunn, R. L. (1991) Polymeric Matrices. In: *ACS Symposium Series*. American Chemical Society, ISBN 9780841213258, Washington DC, USA.
- Griffith, L. G. & Grodzinsky, A. J. (2001) Advances in Biomedical Engineering. *The Journal of the American Medical Association*, Vol.285, No.5, pp.556-61, ISSN 0098-7484
- Gunatillake, P. A. & Adhikari, R. (2003). Biodegradable Synthetic Polymers for Tissue Engineering. *European Cells and Materials*, Vol.5, pp.1-16, ISSN 14732262
- Harley, B. A. C.; Kim, H.-D.; Zaman, M. H.; Yannas, I. V.; Lauffenburger, D. A. & Gibson, L. J. (2008) Microarchitecture of Three-Dimensional Scaffolds Influences Cell Migration Behavior via Junction Interactions. *Biophysical Journal*, Vol.95, No.8, pp.4013-4024, ISSN 1542-0086
- Holland, S. J. & Tighe, B. J. (1992). Advances in Pharmaceutical Science, In: *Biodegradable Polymers*, London, 101 - 165, Academic Press London: London, ISBN 978-1859571187
- Hollister, S. J.; Maddox, R.D. & Taboas, J. M. (2002). Optimal Design and Fabrication of Scaffolds to Mimic Tissue Properties and Satisfy Biological Constraints. *Biomaterials*, Vol.23, No.20, pp.547-557, ISSN 0142-9612
- Hoque, M. E.; Hutmacher, D. W.; Feng, W.; Li, S.; Huang, M. H.; Vert, M. & Wong, Y. S. (2005). Fabrication Using a Rapid Prototyping System and In Vitro Characterization of PEG-PCL-PLA Scaffolds for Tissue Engineering. *Journal of Biomaterials Science: Polymer*. Vol.16, No.12, pp.1595-610, ISSN 1568-5624
- Hoque, M. E., San, W. Y., Wei, F., Li, S., Huang, M.-H., Vert, M. & Hutmacher, D. W. (2008) Processing of Polycaprolactone and Polycaprolactone-Based Copolymers into 3D Scaffolds, and Their Cellular Responses. *Tissue Engineering Part A*, Vol.15, No.10, pp.3013-3024, ISSN 1937-3341
- Huang, A. H.; Farrell, M. J. & Mauck, R. L. (2010). Mechanics And Mechanobiology of Mesenchymal Stem Cell-Based Engineered Cartilage. *Journal of Biomechanics*, Vol.43, No.1, pp.128-36.
- Joseph, J. G. (2006). Polymers For Tissue Engineering, Medical Devices, and Regenerative Medicine. Concise General Review of Recent Studies. *Polymers for Advanced Technologies*, Vol.17, pp.395-418, ISSN 1042-7147
- Joseph, P. V. & Robert, L. (1999). Tissue Engineering: The Design and Fabrication of Living Replacement Devices for Surgical Reconstruction and Transplantation. *Lancet*, Vol.354, pp.32-34, ISSN 0140-6736

- Ke, C. & William, S. K. (2010). Exploring Cellular Adhesion and Differentiation in a Micro-/Nano-Hybrid Polymer Scaffold. *Biotechnology Progress*, Vol.26, No.3, pp.838-846, ISSN 1520-6033
- Lacroix, D. & Prendergast, P. J. (2002). A Mechano-Regulation Model for Tissue Differentiation During Fracture Healing: Analysis of Gap Size and Loading. *Journal of Biomechanics*, Vol.35, No.9, pp.1163-1171, ISSN 0021-9290
- Lalan, B. A. S.; Pomerantseva, M. D. I.; Joseph, P. & Vacanti, M. D. (2001). Tissue Engineering and its Potential Impact on Surgery. *World Journal of Surgery*, Vol.25, No.11, pp.1458-1466, ISSN 0364-2313
- Lebourg, M.; Serra, R. S.; Estelles, J. M.; Sanchez, F. H.; Ribelles, J. L. G. & Anton, J. S. (2008). Biodegradable Polycaprolactone Scaffold with Controlled Porosity Obtained by Modified Particle-Leaching Technique. *Journal of Materials Science*, Vol.19, No.5, pp.2047-2053, ISSN 0022-2461
- Legault, M. (March 2008). Rapid Manufacturing, Part I: The Technologies In Technology, In *Composite World*, 8.03.2008, Available from <http://www.compositesworld.com/articles/rapid-manufacturing-part-i-the-technologies>
- Leong, K. F. (2003). Solid Freeform Fabrication of Three-Dimensional Scaffolds For Engineering Replacement Tissues and Organs. *Biomaterials*, Vol.24, No. 13, pp.2363-2378, ISSN 0142-9612
- Madhally, S. V. & Matthew, H. W. T. (1999). Porous Chitosan Scaffold for Tissue Engineering. *Biomaterials* Vol.20, No.12, pp.1133-1142, ISSN 0142-9612
- Maher, P. S.; Keatch, R. P.; Donnelly, K. & Mackay, R. E. (2009a). Construction of 3D Biological Matrices Using Rapid Prototyping Technology. *Rapid Prototyping Journal*, Vol.15, No.3, pp.204-210, ISSN 1355-2546.
- Maher, P. S.; Keatch, R. P.; Donnelly, K. & Paxton, J. Z. (2009b). Formed 3D Bio-Scaffolds via Rapid Prototyping Technology. 4th European Conference of The International Federation for Medical and Biological Engineering. Antwerp, Belgium. Vol.22, No.17, pp.2200-2204.
- Mastrogiamaco, M.; Muraglia, A.; Komlev, V.; Peyrin, F.; Rustichelli, F.; Crovace, A. & Cancedda, R. (2005). Tissue Engineering of Bone: Search for a Better Scaffold. *Orthodontics & Craniofacial Research*, Vol.8, No.4, pp.277-284, ISSN 1601-6343
- Moroni, L.; Schotel, R.; Sohler, J.; De Wijn, J. R. & Van Blitterswijk, C. A. (2006). Polymer Hollow Fiber Three-Dimensional Matrices with Controllable Cavity and Shell Thickness. *Biomaterials*, Vol.27, No.35, pp.5918-5926, ISSN 0142-9612
- Olivares, A. L.; Marsal, È.; Planell, J. A. & Lacroix, D. (2009). Finite Element Study of Scaffold Architecture Design and Culture Conditions for Tissue Engineering. *Biomaterials*, Vol.30, No.30, pp.6142-6149, ISSN 0142-9612
- Park, J. & Lakes, R. S. (2007) *Biomaterials : An Introduction* (Third Edition), Springer Sciences-Business Media, 978-0-387-37879-4, New York Usa
- Piao, L.; Dai, Z.; Deng, M.; Chen, X. & Jing, X. (2003). Synthesis and Characterization of PCL/PEG/PCL Triblock Copolymers By Using Calcium Catalyst. *Polymer*, Vol.44, No.7, pp.2025-2031, ISSN 0032-3861

- Pinar, Y.; Rui, A. S.; Rui, L. R. & Nesrin, H. V., H (2008). 3D Plotted PCL Scaffolds For Stem Cell Based Bone Tissue Engineering. *European symposium on biopolymers*, Vol.269, pp.92-99.
- Puppi, D.; Chiellini, F.; Piras, A. M. & Chiellini, E. (2010). Polymeric Materials for Bone and Cartilage Repair. *Progress In Polymer Science*, Vol.35, No.4, pp.403-440, ISSN 0079-6700
- Sonal, L. (2001). Tissue Engineering and Its Potential Impact on Surgery. *World Journal Of Surgery*, Vol.25, No.11, pp.1458-66, ISSN 0364-2313
- Starly, B.; Lau, W.; Bradbury, T. & Sun, W. (2006). Internal Architecture Design and Freeform Fabrication of Tissue Replacement Structures. *Computer-Aided Design*, Vol.38, No.2, pp.115-124, ISSN 0010-4485
- Sun, W.; Starly, B.; Nam, J. & Darling, A. (2005). Bio-Cad Modeling and Its Applications In Computer-Aided Tissue Engineering. *Computer-Aided Design*, Vol.37, No.11, pp.1097-1114, ISSN 0010-4485
- Tan, J. Y., Chua, C. K. & Leong, K. F. (2010) Indirect fabrication of gelatin scaffolds using rapid prototyping technology. *Virtual and Physical Prototyping*, Vol. 5, No.1, pp.45-63, ISSN 1745-2759
- Tanaka, M. & Sackmann, E. (2005). Polymer-Supported Membranes As Models of The Cell Surface. *Nature*, Vol.437, pp.656-663, ISSN 0028-0836
- Tay Francis E.H., M.A. Manna & L.X. Liu. (2002) A Novel Method of Manufacturing Prosthetic Sockets By Fused Deposition Modelling And CAD/CAM Technology. *Rapid Prototyping*, Vol. 8, No. 4, pp.258-262, ISSN 1544-9491
- Tezcaner, A.; Köse, G. & Hasırcı, V. (2002). Fundamentals of Tissue Engineering: Tissues and Applications Technology and Health Care, *IOS Press*, Vol.10, No.3-4, pp.203-216, ISSN 0928-7329
- Tjong, S. C. (2006). Structural and Mechanical Properties of Polymer Nanocomposites. *Materials Science and Engineering: R: Reports*, Vol.53, No.3-4, pp.73-197, ISSN 0927-796X
- Thomson, R. C., Shung, A. K., Yaszemski, M. J. & Mikos, A. G. (2000) Polymer Scaffold Processing. In : *Principles of Tissue Engineering*. Second Edition Lanza, R., Langer, R. & Vacant, J. P ed. California, 978-0124366305, Academic Press.
- Van Cleynenbreugel, T.; Schrooten, J.; Van Oosterwyck, H. & Vander Sloten, J. (2006). Micro-Ct-Based Screening of Biomechanical And Structural Properties of Bone Tissue Engineering Scaffolds. *Medical And Biological Engineering And Computing*, Vol.44, No.7, pp.517-525, ISSN 0140-0118
- Xiong, Z.; Yan, Y.; Wang, S.; Zhang, R. & Zhang, C. (2002). Fabrication of Porous Scaffolds For Bone Tissue Engineering Via Low-Temperature Deposition. *Scripta Materialia*, Vol.46, No.11, pp.771-776, ISSN 1359-6462
- Yang, S. F.; Du, Z. H. & Leong, K. F. (2001). The Design of Scaffolds for Use In Tissue Engineering. Part I. Traditional Factors. *Tissue Engineering*, Vol.7, No.6, pp.679-89, ISSN 1937-3368
- Yeong, W.-Y.; Chua, C.-K.; Leong, K.-F. & Chandrasekaran, M. (2004). Rapid Prototyping In Tissue Engineering: Challenges and Potential. *Trends In Biotechnology*, Vol.22, No.12, pp.643-652, ISSN 0167-7799

Zhensheng, L.; Jonathan, G.; Hong, C. M.; Ashleigh, C. & Miqin, Z. (2008). On-Site Alginate Gelation For Enhanced Cell Proliferation and Uniform Distribution In Porous Scaffolds. *Journal of Biomedical Materials Research Part A*, Vol.86, No.2, pp.552-559, ISSN 1549-3296

IntechOpen

IntechOpen



Rapid Prototyping Technology - Principles and Functional Requirements

Edited by Dr. M. Hoque

ISBN 978-953-307-970-7

Hard cover, 392 pages

Publisher InTech

Published online 26, September, 2011

Published in print edition September, 2011

Modern engineering often deals with customized design that requires easy, low-cost and rapid fabrication. Rapid prototyping (RP) is a popular technology that enables quick and easy fabrication of customized forms/objects directly from computer aided design (CAD) model. The needs for quick product development, decreased time to market, and highly customized and low quantity parts are driving the demand for RP technology. Today, RP technology also known as solid freeform fabrication (SFF) or desktop manufacturing (DM) or layer manufacturing (LM) is regarded as an efficient tool to bring the product concept into the product realization rapidly. Though all the RP technologies are additive they are still different from each other in the way of building layers and/or nature of building materials. This book delivers up-to-date information about RP technology focusing on the overview of the principles, functional requirements, design constraints etc. of specific technology.

How to reference

In order to correctly reference this scholarly work, feel free to copy and paste the following:

Md. Enamul Hoque and Y. Leng Chuan (2011). Desktop Robot Based Rapid Prototyping System: An Advanced Extrusion Based Processing of Biopolymers into 3D Tissue Engineering Scaffolds, Rapid Prototyping Technology - Principles and Functional Requirements, Dr. M. Hoque (Ed.), ISBN: 978-953-307-970-7, InTech, Available from: <http://www.intechopen.com/books/rapid-prototyping-technology-principles-and-functional-requirements/desktop-robot-based-rapid-prototyping-system-an-advanced-extrusion-based-processing-of-biopolymers-i>

INTECH
open science | open minds

InTech Europe

University Campus STeP Ri
Slavka Krautzeka 83/A
51000 Rijeka, Croatia
Phone: +385 (51) 770 447
Fax: +385 (51) 686 166
www.intechopen.com

InTech China

Unit 405, Office Block, Hotel Equatorial Shanghai
No.65, Yan An Road (West), Shanghai, 200040, China
中国上海市延安西路65号上海国际贵都大饭店办公楼405单元
Phone: +86-21-62489820
Fax: +86-21-62489821

© 2011 The Author(s). Licensee IntechOpen. This chapter is distributed under the terms of the [Creative Commons Attribution-NonCommercial-ShareAlike-3.0 License](#), which permits use, distribution and reproduction for non-commercial purposes, provided the original is properly cited and derivative works building on this content are distributed under the same license.

IntechOpen

IntechOpen